

dpl

R-548

SENSORY, DECISION AND CONTROL SYSTEMS
APRIL TO JULY 1966

by
Louis L. Sutro, et al.

November 1966

FOR OFFICIAL USE ONLY

This document has been prepared for Instrumentation Laboratory use and for controlled external distribution. Reproduction or further dissemination is not authorized without express written approval of M.I.T. This document has not been reviewed by the Directorate for Security Review, OSD, and therefore, is not for public release.

FACILITY FORM 602

N67-25955
(ACCESSION NUMBER)

50
(PAGES)

CR 83892
(NASA CR OR TMX OR AD NUMBER)

(THRU)

1
(CODE)

10
(CATEGORY)

**INSTRUMENTATION
LABORATORY** ●

MASSACHUSETTS INSTITUTE OF TECHNOLOGY
Cambridge 39, Mass.

R-548

**SENSORY, DECISION AND CONTROL SYSTEMS
APRIL TO JULY 1966**

by

Louis L. Sutro, et al.

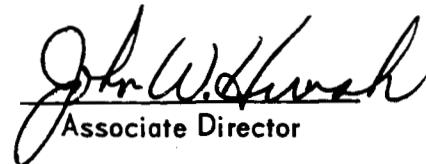
November 1966

A report of work performed from
April 16 to July 15, 1966 under
NASA Contract NSR 22-009-138,
and from October 1, 1965 to
July 15, 1966 under Air Force
Contract AF 04(695)-917.

**INSTRUMENTATION LABORATORY
MASSACHUSETTS INSTITUTE OF TECHNOLOGY
CAMBRIDGE, MASSACHUSETTS**

*Prepared for publication by Jackson & Moreland
Division of United Engineers & Constructors, Inc.*

Approved


Associate Director

Approved


Deputy Director

ACKNOWLEDGEMENT

Sections 1, 2, 3 and 5 and subsection 4.7 were prepared under the auspices of DSR Project 55-25700, sponsored by the Bioscience Division of the National Aeronautics and Space Administration through Contract NSR-22-009-138. Sections 4 and 6, with the exception of subsection 4.7, were prepared under the auspices of DSR Project 52-25600, sponsored by the Space Systems Division, U. S. Air Force Systems Command through Contract AF 04(695)-917.

Major contributions to the program have been made by consultants to the Laboratory, by members of the Sensory, Decision and Control Systems (SDCS) Group of the Longspur Section of the Instrumentation Laboratory and other members of the Longspur Section:

Consultants –

Dr. Warren S. McCulloch
Dr. William L. Kilmer
Dr. Carl Sagan

The SDCS Group –

Jay Blum – Staff Member
Richard Catchpole – Research Assistant
Jerome L. Krasner – Staff Member
Dr. Roberto Moreno-Diaz – Staff Member
David Peterson – Research Assistant
Louis Sutro – Assistant Director
David Tweed – Staff Member

Other Members of the Longspur Section –

Joseph Convers – Staff Member

Editorial assistance was provided by David Lampert, a research assistant, who joined the SDCS Group after the period of this report.

ABSTRACT

The quarter reported here for the NASA contract, and the longer period reported for the Air Force contract, saw the development of two system concepts for the transmission of video data from a remote location to Earth. In the simpler system, a stereoscopic outline together with other data such as reflectance and possibly the texture of objects will be transmitted to Earth. The objects considered are those larger than a predetermined size and within a predetermined range. From the stereoscopic outlines presented to the operator on Earth he will decide what objects he would like pictured in full TV frames and order these transmitted.

In the more elaborate system, TV cameras will be carried on a vehicle and the direction in which the vehicle moves will be chosen by an onboard decision computer. Perceptual decisions may also be made to identify objects whose characteristics have been reported to Earth and whose value to the Earth observer has been communicated back to the perceptual computer. The assembly of cameras, perceptual computer, decision computer and vehicle is called a robot.

Photosensors for this robot are television cameras, the first models of which have been tested under computer control. A model of both the perceptual computer and the decision computer has been simulated. It consists of 12 modules, each of which makes an initial guess as to what the response to incoming data should be. Each takes the data from all other modules and combines it in a nonlinear fashion with the data coming directly into it to arrive at a mixed guess as to what act should be performed. When 60% of the modules vote 0.5 probability for one act, that act is performed. Convergence to a satisfactory decision took from 5 to 25 time steps.

The model of the frog's retina previously reported is here extended to that part of the brain, called the tectum, where the frog begins to respond to objects detected by the retina.

TABLE OF CONTENTS

Section	Page
1 INTRODUCTION	1
1.1 Goal	1
1.2 Approaches to the Goal	1
1.3 Increased Scope of the Reports	2
1.4 Aid to be Provided an Earth Biologist	2
1.5 Transmission of Video Data between Mars and Earth	2
1.6 Contacts with Jet Propulsion Laboratory	3
1.7 Research Into the Nature of Vision	3
2 SYSTEM DESIGN	4
2.1 Camera-Computer System	4
2.2 Robot-Computer System	5
2.3 The Robot	5
2.4 A Vehicle for Exploring Mars	7
2.5 Display Subsystem	7
3 VISUAL SUBSYSTEM	9
3.1 General	9
3.2 Requirements for Camera A	9
3.3 Experimental Camera A	9
3.4 Experimental Camera C	11
3.5 Experimental Camera Assemblies B, C, D and E	11
3.6 Visual Decision Computer	11
4 VIDICON CAMERA DEVELOPMENT AND INVESTIGATIONS OF SOLID-STATE SENSORS	14
4.1 Camera A: Choice of Vidicon and Design Description	14
4.2 Choice of Supplier	15
4.3 Method of Scanning	15
4.4 Vidicon Circuitry	15
4.5 Improved Deflection Amplifiers	15
4.6 Operation of Camera Under Computer Control	16
4.7 Solid State Sensors	17
5 THE DECISION SUBSYSTEM	19
5.1 Goal	19
5.2 Previous Descriptions	19
5.3 Simulation	20
5.4 Computer Design	20
5.5 Operation in General	21

TABLE OF CONTENTS (Cont.)

<u>Section</u>	<u>Page</u>
5.6 Definitions	23
5.7 Detailed Operation	24
5.8 Structure of a Module	25
5.9 The A-Part of Each Module	25
5.10 The B-Part of Each Module	25
 6 CONCEPTUAL MODEL OF THE FROG'S TECTUM	 30
6.1 Introduction	30
6.2 Neurophysiological Basis of the Model	32
6.3 Conceptual Model	35
6.4 Interaction Process A (Facilitation)	36
6.5 Interaction Process B (Adaptation)	37
6.6 Interaction Processes C and D	38
(Maximum-activity selection and distribution)	
6.7 Parameters of Types N and S Neurons	38
6.8 Equivalent Circuit of a Group of Tectal Cells	39
6.9 Discussion	40
 Appendix	
A NOTE TO SECTION 5: IMPLEMENTATION OF THE A-PART OF A DECISION-SYSTEM MODULE USING THRESHOLD LOGIC.	41

SECTION 1

INTRODUCTION

by
Louis Sutro

1.1 Goal

It is the aim of this program to provide both NASA and the U. S. Air Force with sensory-decision-control systems founded within the present state of the art and yet capable of object recognition in space. At the present, although it is known how to send television pictures from remote locations to Earth, the transmission time per full picture encumbers any earth-bound control system. Consequently, automatic ways are being explored to extract from a scene features such as the outlines, locations, and textures of objects. These features will be communicated to Earth and will provide a scientist or military officer with information sufficient for a decision as to which TV pictures should be sent from the remote location. Transmitted back to the remote location, these decisions will then command the TV camera.

This is the first system under development. In a later system, the camera will be mounted on a vehicle and the on-board computers will extract features to decide where the vehicle should go and possibly which TV frames should be sent to Earth. The assembly of camera, computer, and vehicle is referred to as a robot.

1.2 Approaches to the Goal

Two approaches are being followed. One is to increase our understanding of animal sensory, decision, and control systems by designing models of these systems that can be built out of light, portable hardware. This is accomplished through research.

The other approach is to design semiautomatic chains of television cameras and computers for remote operation, as well as displays for Earth operation, so that scientists or military officers on Earth may more easily carry out remote explorations. This approach is development.

1.3 Increased Scope of the Reports

This report covers work performed for both the Bioscience Programs of the NASA Office of Space Science and Applications and the U. S. Air Force Space Systems Division. The former work is reported in Sections 2, 3, 5 and subsection 4.7; the latter in Sections 4 and 6.

The descriptive title of this series of reports has lengthened as the scope of the work has broadened: The initial report⁽¹⁾ referred only to sensors, the next report⁽²⁾ included control systems, and this report includes decision systems. Reference 3 has a title different from the others because it was presented as a paper at a conference.

1.4 Aid to be Provided an Earth Biologist

The task for the NASA Office of Space Science and Applications is to develop means of transmitting from Mars to Earth the kind of information that will assist an Earth biologist in search for life on Mars. It is planned to make available to him, when he wishes, entire TV frames with 64 levels of gray, although during most of the mission it would be preferable to limit transmission to outlines of objects and indications of their surface texture. So that he may still be able to judge where these objects are, their outlines will be presented stereoscopically. Only when the outline or texture of an object suggests life would it be recommended that the Earth biologist request the full TV frame of which the system is capable.

If the television cameras on Mars can be carried by a vehicle, the range of exploration will be greatly increased. Already, under contract to Jet Propulsion Laboratory, similar vehicles have been developed for the exploration of the moon. Assuming that such a vehicle can be provided for the Mars mission, it appears to fall to us, as designers of its "eyes", to design also a means of guiding a vehicle in response to what is seen.

As the eyes, means of locomotion, and ability to make decisions are put together, a robot emerges that is capable of performing by itself tasks as complex as the avoidance of obstacles. Eventually it might also select the views to be reported in full TV detail to Earth, although the Earth operator should still be able to override the Mars decision. Thus, the possibility is opened for continual searching on Mars without waiting for instructions from Earth.

1.5 Transmission of Video Data between Mars and Earth

The problem of transmitting video data from Mars was illustrated by the Mariner IV spacecraft, which flew by Mars in July, 1965. Each of its 22 pictures comprised 200 by 200 spots and each spot was represented by 6 bits. Transmission of one of these pictures (2.4×10^5 bits) required eight hours. The number of bits transmitted per day was three times this, or 7.2×10^5 .

John J. Mahoney of the Avco Corporation estimates that in the 1970's, again using a direct link, a soft lander on Mars will be able to transmit up to 10^7 bits per day,⁽⁴⁾ which is only an order of magnitude better than the Mariner IV system. Moreover, this assumes an antenna 3 feet in diameter aimed at a beacon tone-transmitted from Earth. Thus the problem of transmission is so great that means should be found to equip the Mars system with some ability to decide what pictures shall be sent and what actions shall be taken.

1.6 Contacts with Jet Propulsion Laboratory

This period was also devoted to tying our objectives to the long-range planning of the Jet Propulsion Laboratory of the California Institute of Technology. To attain this end, members of our staff spent seven man-days conferring with members of the staff of the Jet Propulsion Laboratory, with the result that we now know what has been done to prepare for voyages to Mars and when such voyages are expected to take place. Further examples of the fruits of the new acquaintances are additional knowledge of vidicons, reported in subsection 4.1, and acquaintance with vehicles for lunar and planetary landing, mentioned in subsection 1.4.

1.7 Research Into the Nature of Vision

Section 6 extends the model of the frog's visual system^(5,6) by including that part of the brain, called the tectum, where cells previously modeled terminate. Tectal cells interpret incoming contour and movement signals according to the animals innate preferences. In the opinion of Dr. McCulloch, tectal cells send signals to the tiny cerebellum (which controls eye movement), to nuclei that control the tongue and jaws, through the thalamus to what little cortex the frog has and to the spinal cord. In his opinion the great bulk of tectal cell signals go to the reticular formation, a model of which is presented in Section 5.

SECTION 2

SYSTEM DESIGN

by

Louis Sutro, William Kilmer and Warren McCulloch

2.1 Camera-Computer System

The first kind of system mentioned in subsection 1.1 is shown in Fig. 2-1

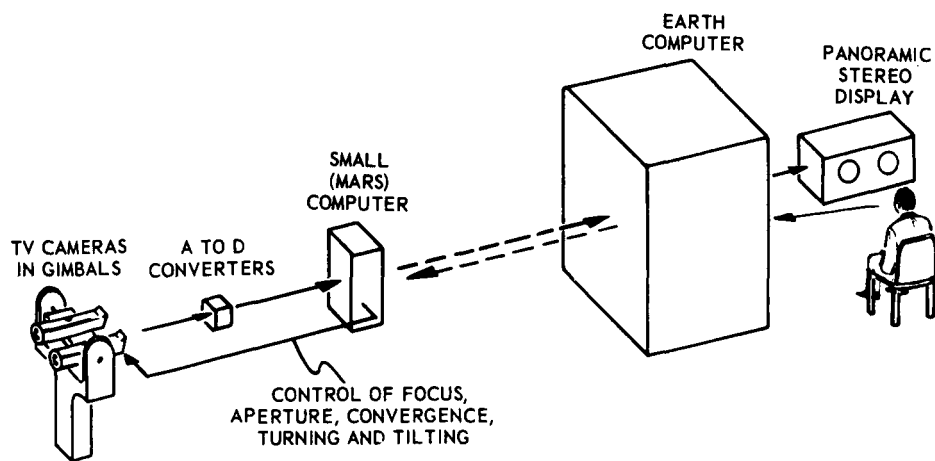


Fig. 2-1. Block diagram of Mars-Earth camera computer system.

as it might be employed in the search for life on Mars. At the left is a stereoscopic pair of TV cameras, at the right a small computer. Further to the right, across 35 million miles or more of space, is the Earth computer and the display provided to a scientist there. He would see the outlines and textures of objects viewed by the cameras, decide what might indicate the presence of life, and request TV pictures of these. He would communicate his decision to the Earth computer, which in turn would communicate it to the Mars computer, which would command the cameras.

In the system as first conceived, the Earth computer would perform such detailed operations and analyses on the digitized pictorial data as were performed

on the television pictures transmitted from the Ranger and Mariner spacecraft⁽¹⁸⁾. First, the picture (or pictorial data) is clarified by the correction of distortions which adversely affect geometric, photometric and frequency fidelity. Then, the cleaned-up, enhanced picture is used both by the computer for further interpretive and statistical analyses as well as by the scientist for visual photo interpretation. The data processing involved was handled in the Ranger and Mariner system by an IBM 7094 at Jet Propulsion Lab and is expected to be handled in the Mars system by the large computer illustrated in Fig. 2-1.

Continued study of this first kind of system has indicated that for automatic direction of the cameras on Mars, cleaning-up and analysis will have to be performed in the Mars computer.

2.2 Robot-Computer System

In the more elaborate system mentioned in subsection 1.1, a vehicle equipped with cameras and a computer would search for evidence of life in accordance with general instructions programmed into the computer. The scientist on Earth would communicate to the robot in any of the following three ways:

1. A command,
2. A question or call for information transmission
3. A statement (information) .

These are three moods of language: imperative, interrogative and declarative.

2.3 The Robot

Figure 2-2 is a block diagram of robot operation as presently conceived. At the center left approximately 500 lines connect the sensors with approximately 50 modules of the decision computer in a several-to-several fashion. At top left the three modes of communication from Earth, listed in subsection 2.2 are shown entering the communications box, from which come replies in the form of statements, processed and unprocessed pictures. Through this box the General Problem Solver (GPS) at the top establishes links to and from the decision computer, to and from the Earth station, to the sensors, and from the effectors. The connections from the effectors are feedbacks to the GPS and the decision computer. The acts, shown at the right, are combinations of programs to process a picture, operate wheel motors, operate camera platform, operate arm and hand, etc. Other channels are assumed, e. g. , servo on something in the visual field, servo hand and arm. The decision computer is organized at the block level so that sensory data enters at the left, effector action is controlled at the right.

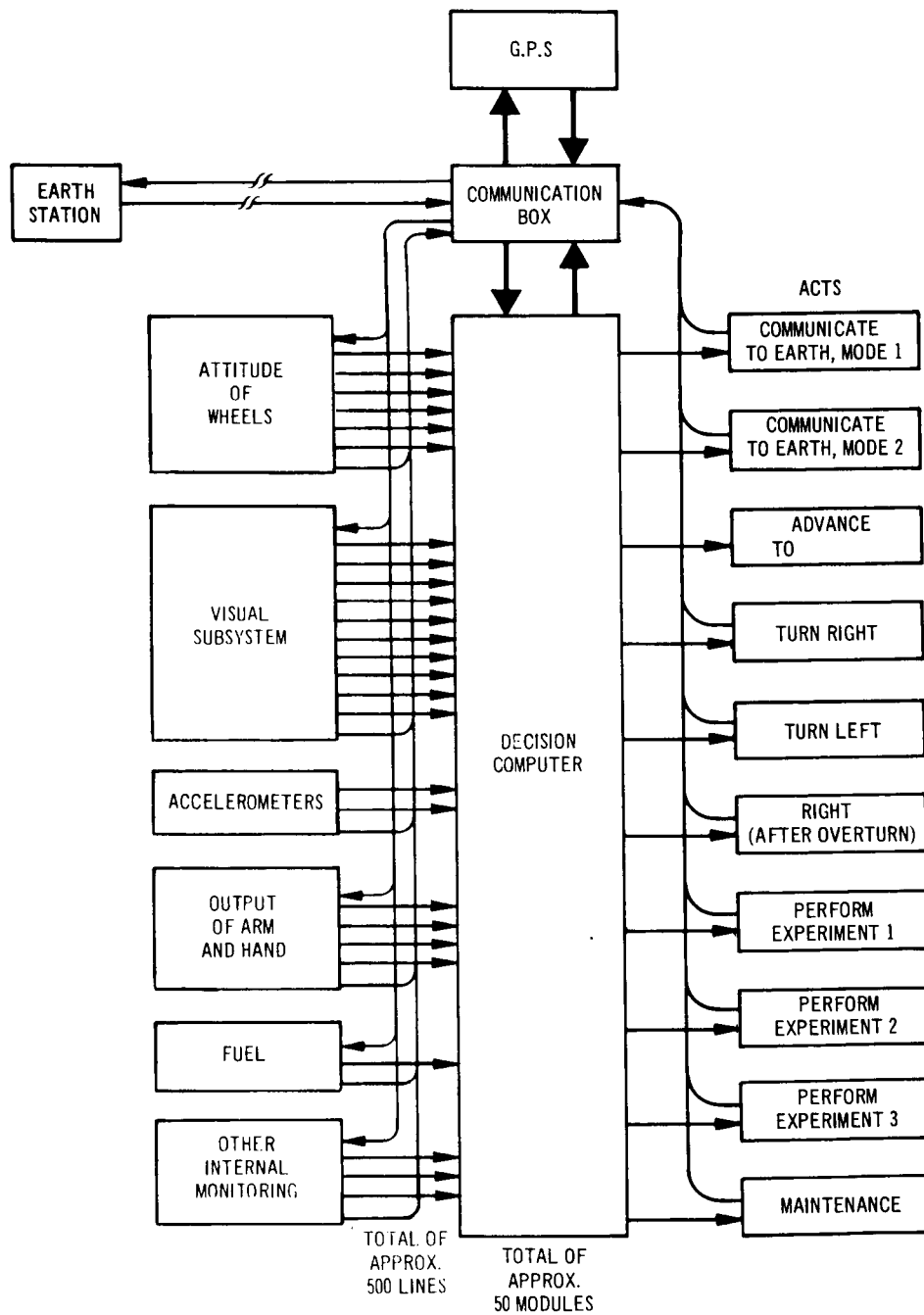


Fig. 2-2. Block diagram of proposed robot operation.

All input lines will be monitored continually, the memory will be moderate in size, and the decision will be made quickly. The GPS will make possible goal-seeking behavior by solving problems on simple models of the environment. For example, suppose the robot has been commanded to a position 10 meters north and it has encountered an obstruction along the way. The GPS will direct the robot in an alternate direction, say east, until it can get around the obstruction. Then the GPS will direct the robot to close on its objective.

2.4 A Vehicle for Exploring Mars

Self-propelled vehicles for extra-terrestrial exploration have been built by Bendix⁽⁷⁾ and General Motors⁽⁸⁾. Both were intended to be carried to the moon by a surveyor spacecraft. Both were designed to carry a stereo television camera and to be guided by a remote operator looking at a stereo display.

The Bendix vehicle is designed to be operated by four caterpillar treads. The General Motors vehicle, as shown in Fig. 2-3, has six wheels separately driven and servo-controlled to permit maneuvering between obstacles. The chassis has been so designed that it can move over terrain that includes objects 1-1/2 wheel diameters high. This flexibility has been achieved by an articulated chassis. Wheels are of covered wire and thus do not have to be inflated.

If either vehicle is used in the proposed robot, the television camera will be replaced by an assembly of cameras in gimbals to be known as camera assembly E. The flexibility of the chassis will then need to be reduced so that the stereo base (line between the optical centers of the two cameras) can be maintained in a horizontal position during camera operation.

2.5 Display Subsystem

Determination of the presence of life on Mars can be made only by biologists interpreting data communicated to them by remote sensors. Principal forms of this data are expected to be either stereo photographs or stereoscope displays.

For the simpler of the two systems proposed in this report, the Earth scientist may find the display shown in Fig. 2-1 to be sufficient. For the more elaborate system, however, it appears desirable that he be surrounded by photographs or displays so that he can consider every possible direction before ordering the robot in one of them. A form of stereo photograph that could serve this purpose is the Vectograph, which when seen through appropriate Polaroid glasses provides a stereo view.

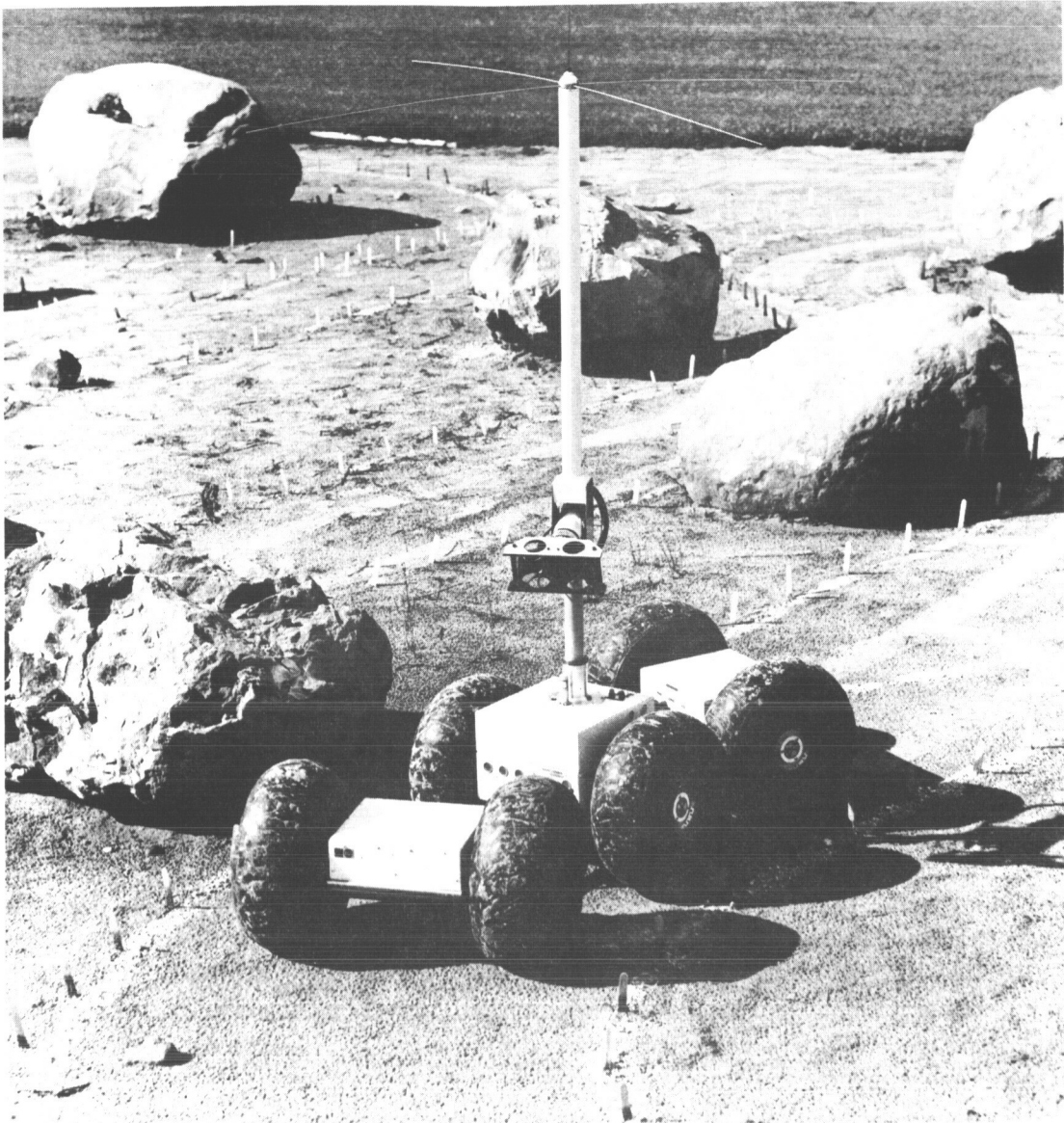


Fig. 2-3. General Motors vehicle on test grounds.

SECTION 3

VISUAL SUBSYSTEM

by

Louis Sutro and William Kilmer

3.1 General

For the simpler system mentioned in subsection 1.1, the visual subsystem consists of the cameras and Mars computer pictured in Fig. 2-1. For the more elaborate system, it consists also of a vehicle and a visual decision computer.

Two approaches are being taken to the design of the visual subsystem. One is the simulation of animal visual systems described in previous reports^(1,2,3) and in Section 6. The other is engineering design. This section and Section 4 are of the latter nature.

3.2 Requirements for Camera A

- a. The equipment is to be capable of scanning scenes for computer analysis.
- b. To preserve the usefulness of the vidicon photoconductive film, it shall always be scanned over its largest useful area. For a one-inch tube this is approximately 0.5 inch by 0.5 inch.
- c. The number of scan lines and number of positions per line shall both be either 256 or 512.
- d. Each video sample is to be quantized to six bits.

3.3 Experimental Camera A

Camera A, shown in Fig. 3-1, consists of a vidicon surrounded by a video amplifier on the tripod at the left; deflection circuits in the top two panels in the rack at the right and, at the bottom of the rack; power supplies and controls. Two identical sets of power supplies and controls were placed in the lower part of the rack in preparation for Camera B.

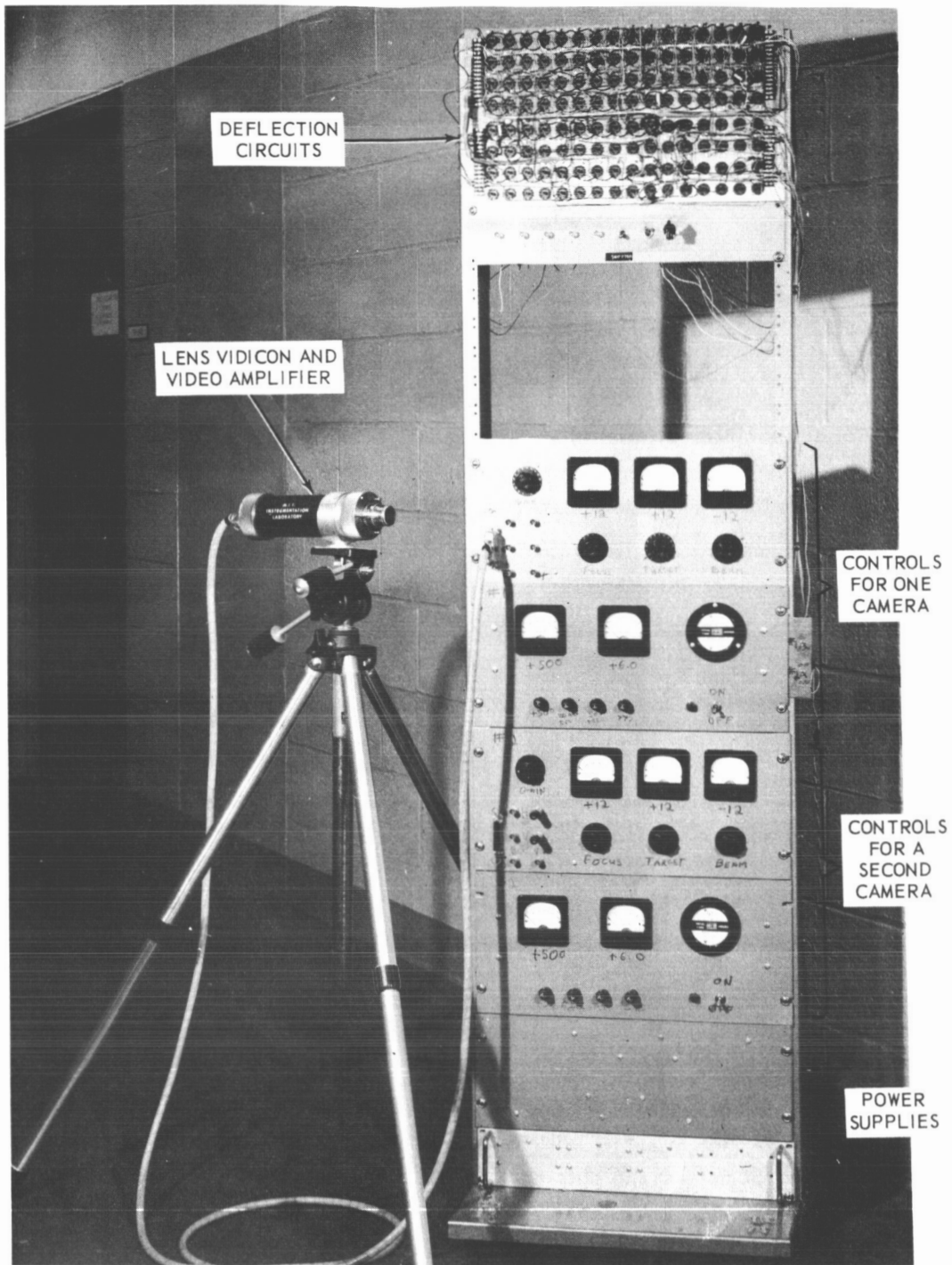


Fig. 3-1. Camera A, voltage controls and power supplies.

3.4 Experimental Camera C

A new camera, called Model C, will replace the Model A and be employed in Camera Assemblies C and D. Advantages of the new camera include greater bandwidth, DC-coupled blanking during flyback, and an increase in frame rate from 1 frame/3 sec to 7 frames/sec due to better integration of the camera with the A-D converter and computer.

3.5 Experimental Camera Assemblies B, C, D and E

Experimental camera assembly B was planned to include two cameras, both looking at the same scene through a beam splitter, one having a fast response and the other slow. By comparing the outputs of the two cameras, a computer should be able to detect motion. Such a scheme is shown in a proposed model of the frog's retina.⁽⁹⁾ It is not stereoscopic at present.

Experimental camera assemblies C, D and E will be stereoscopic; that is, light will enter along two axes separated by a distance either equal to or greater than that between the human eyes. Camera assembly C (Fig. 3-2) will employ a stereo head on a single camera. The utility of such a system has been demonstrated by motion pictures taken through the stereo head. Since the two optical axes in a stereo head are parallel, the field of view is fairly wide (25°) and the resolution on the face of the camera tube poor. To improve this resolution, the single camera with its stereo head will be replaced, in camera assembly D, by two cameras having narrow acceptance angles and capable of convergence. Each camera can turn through 35° , as shown in Fig. 3-3. The case supporting the two cameras can nod through an angle of 30° .

Camera assembly E is at present an objective: an assembly much more compact than assembly D, it is mounted on three gimbals, the outermost of which will be attached to a vehicle.

3.6 Visual Decision Computer

Figure 3-4 shows how a visual decision computer may determine what is the most likely object observed or pass the question on to the system decision computer. The output of the visual, first-stages computer is the outlines of free-standing objects, their range, their texture, etc. The analog output lines from the visual decision computer indicate degrees to which certain properties are present. Simple properties may indicate the probabilities that they represent different objects. Complicated properties may be formed into object probabilities at a later stage, namely, at the system decision computer, which will command a small number of corresponding acts.

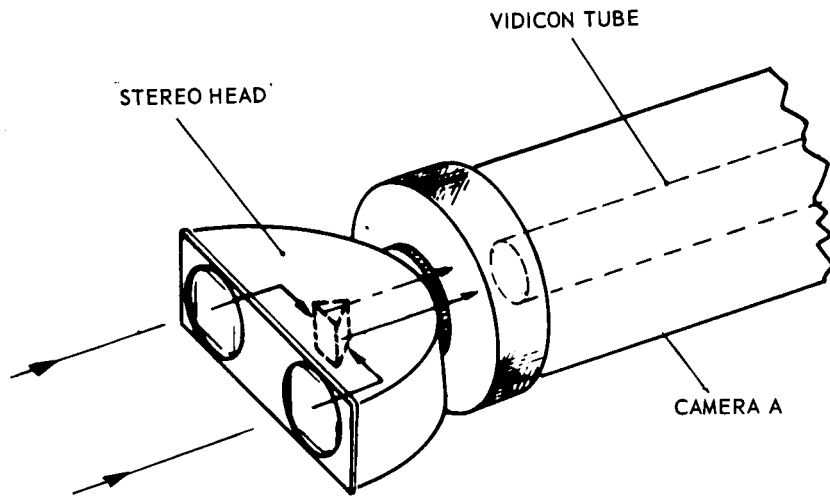


Fig. 3-2. Camera and Stereohead Stereo Head Assembly C as Originally Conceived. Camera A Shown here will be replaced by Camera C.

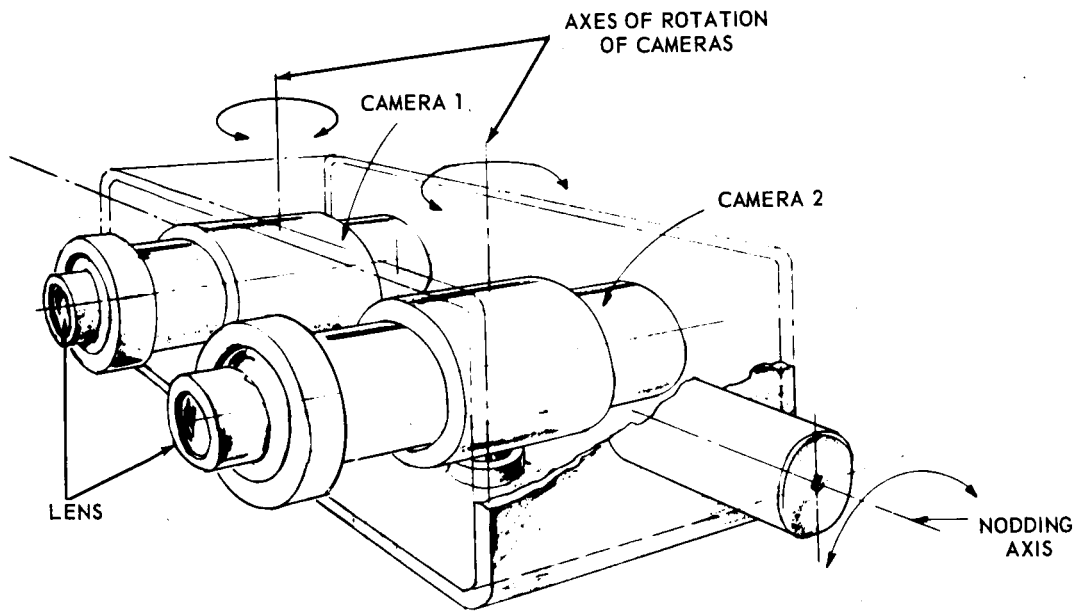


Fig. 3-3. Camera assembly D.

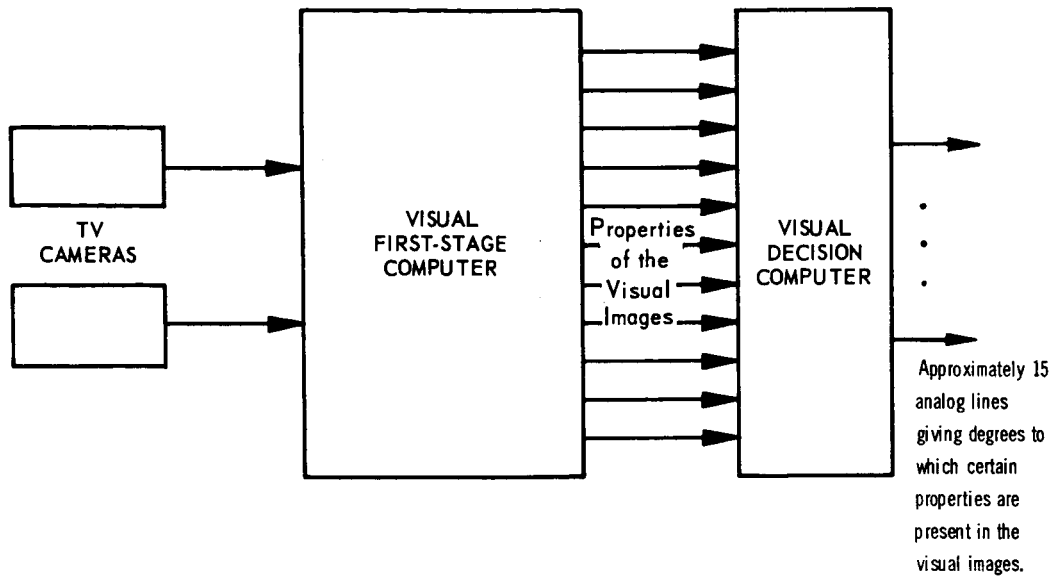


Fig. 3-4. Use of a decision computer in the visual subsystem of a robot.

SECTION 4

VIDICON CAMERA DEVELOPMENT AND INVESTIGATION OF SOLID-STATE SENSORS

by

Richard Catchpole, David Tweed and Louis Sutro

4.1 Camera A: Choice of Vidicon and Design Description

The fast-scan vidicon camera built for experimental camera-computer chain A was designed at the Lincoln Laboratory, M. I. T., to provide a frame time of approximately 1/30 sec, under the constraint that the dwell time* at each position in the raster** was to be at least $2 \mu\text{sec}$. To allow for these specifications, a raster size of 64×256 ($\approx 1.6 \times 10^4$) positions was used. The frequency at which the electron beam advanced was 500,000 Hz,*** the reciprocal of the dwell time.

As plans for camera-computer chain A developed, a larger raster size of 256×256 ($\approx 6.6 \times 10^4$) positions became desirable. Given no change in the dwell time constraint, this fourfold increase in raster size implies a fourfold increase in frame time, which in turn necessitates a fourfold drop in the lower limit of amplifier frequency response.

To meet this requirement, the vidicon amplifier was modified and the fast-scan vidicon was replaced by a slow-scan vidicon. The choice of a slow-scan vidicon was aided by the experience of JPL in using this tube on both their Mariner IV Mars fly-by⁽¹⁰⁾ and the Surveyor lunar landing craft.

Although vidicons magnetically deflected and focussed may have 30 percent higher resolution than their completely electrostatic counterparts, the latter have greater versatility in scanning rate and simplicity of circuitry. This, as well as the design of presently operating equipment, recommended, at least

*The dwell time: The time the vidicon electron beam spends at each position.

**Raster: The pattern produced on the face of the vidicon tube.

***Hertz: The recently adopted international unit for cycles per second.

in the initial experiments, that electrostatic focussing and deflection be used. Although, in our case, the coupling to the deflection plates was poor, these modifications made possible the motion detection experiments to be described in a subsequent report.

4.2 Choice of Supplier

Because of satisfactory previous experience with their products, General Electroynamics was selected as the supplier. This company offers a series of slow-scan electrostatic vidicons ranging in increasing ruggedness from a slow-scan version of the 7522 (to be denoted TD 1343-018), through the TD 1347, to the TD 1343-010 designed for the Mariner missions. The latter is normally supplied with a black level reference and fiducial(reference) markings on its face. The TD 1343-018 (approx \$2,000) appeared adequate for laboratory use, given a dark reference generated by blanking the vidicon during the line flyback.

4.3 Method of Scanning

The existing deflection counter system (Ref. 11), when clocked at a constant rate by the computer, was considered adequate to provide fly-back blanking and end-of-frame signals.

4.4 Vidicon Circuitry

Due to the published limiting resolution of electrostatically deflected and focussed vidicons, there was no point in planning for more than 512 samples per line or lines per frame.

It was decided, as an interim measure, that the video amplifier used in the Lincoln Laboratory DITS system could be modified to meet the requirements given in subsection 4.1 and that optimization of the high frequency cut off, required for a raster measurement of 512×512 , would be attempted later. A basic modification included the increase of the target load resistance permitted by the decrease in importance of high frequency response. The front end of the video amplifier is of excellent low noise design. Blanking during line flyback provided the black reference. All coupling capacitances were increased an order of magnitude.

4.5 Improved Deflection Amplifiers

For the experimental vidicon camera system, a more reliable deflection amplifier was developed to replace that reported in Ref. 11. Within an electrostatic vidicon tube, the deflection electrodes are arranged in pairs which deflect the electron beam in mutually perpendicular directions. (See Fig. 4-1.) Each pair is driven by a deflection amplifier with symmetric output voltages. A typical tube, the General Electroynamics 7522, requires a mean deflection plate

potential of 200 v to 250 v and a potential difference between either pair of up to 60 v. For digital deflection, the amplifiers are driven by low-level voltages from digital-to-analog converters. Continuous horizontal deflection is effected by a ramp generator.

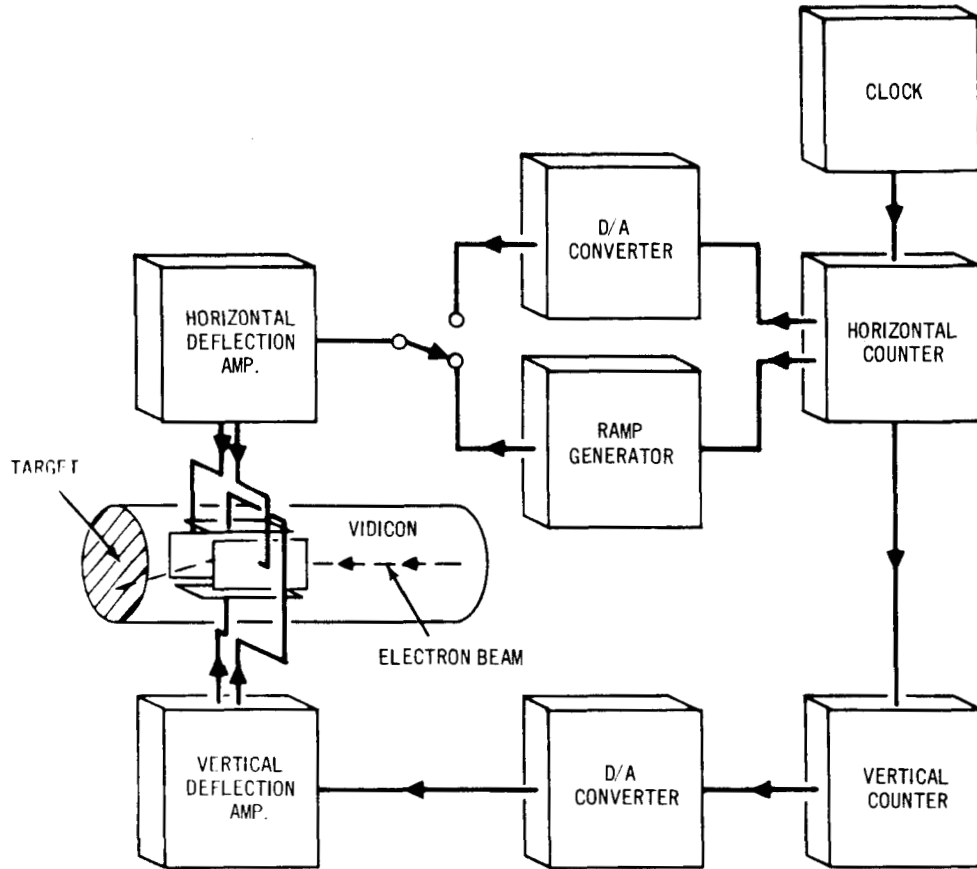


Fig. 4-1. Vidicon deflection system.

The modified Darlington deflection amplifier (Fig. 4-2) uses available voltage supplies and is coupled to the deflection plates by capacitors. Symmetrical negative feedback improves linearity and stabilizes gain. Chains of resistors and zener diodes provide the mean plate voltages. The amplifier rise time is 2 μ secs, a satisfactory value for this experiment.

4.6 Operation of Camera Under Computer Control

The connection of one of the digitally-controlled cameras to M. I. T. 's TX-0 computer permitted an experimental study of motion detection.

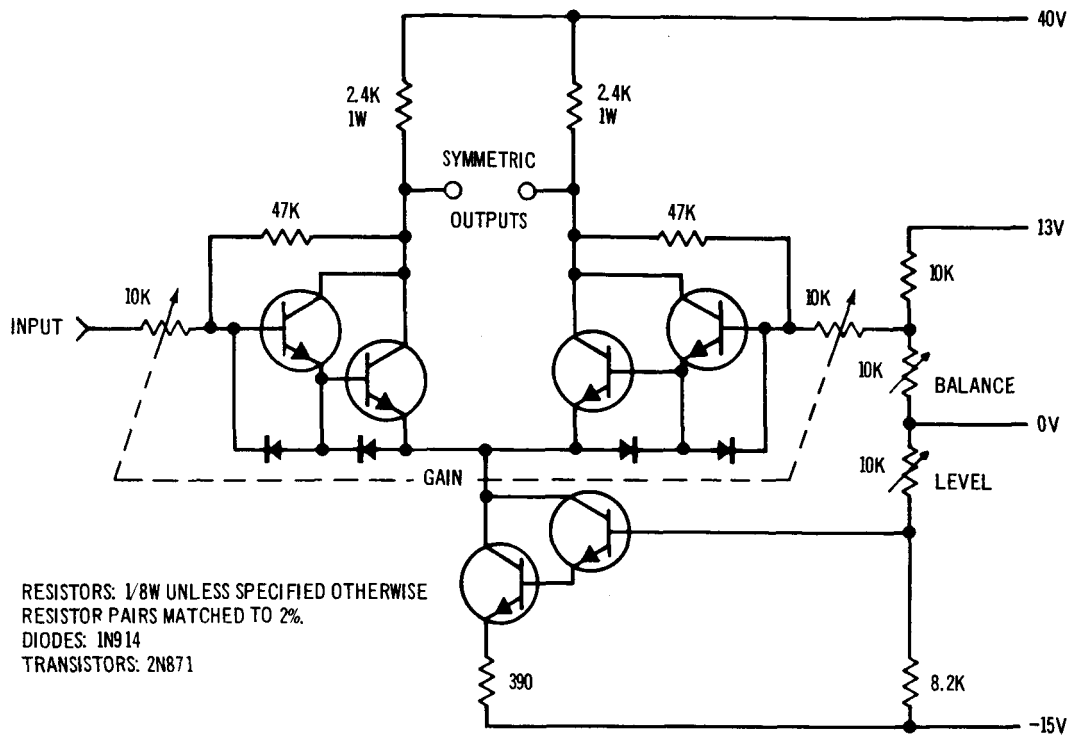


Fig. 4-2. Vidicon deflection amplifier.

The capabilities for data-acquisition of the M. I. T. TX-0 computer and its availability during recent months commended its use on a trial basis for experimenting with and demonstrating visual data acquisition, reduction of visual data to information, and information-processing.

4.7 Solid State Sensors

Visits to Westinghouse's Defense and Space Center, Aerospace Division, Baltimore, Maryland, filled in details of published reports^(12, 13) on the only two-dimensional array of phototransistors now available. An array of phototransistors is being considered because of its smaller size and the discrete position of its photosensitive elements. However, its resolution is poorer and the variation of gamma (see below) over individual units is unknown. For this reason, we have decided to defer procurement of an array until presently-planned tests have been made of the gamma of a representative phototransistor sample.

The gamma of a sensor can be defined as the power to which illumination must be raised in the equation for signal-output current:⁽¹⁴⁾

$$i = k E^\gamma$$

where i is the signal current, k is a constant, E is the illumination on the faceplate of the vidicon, and γ is the exponent commonly referred to as the vidicon gamma. If the gamma of all phototransistors in an array were the same, or if their outputs were to be communicated to Earth, there would be no concern. In the latter case, the gamma of each element of the array could be stored in the Earth computer and used to normalize the returns before interpretation. However, since the goal is to interpret at the remote location through the use of a light portable computer, it is not likely that a large number of gamma values can be stored. Only if gamma is uniform over the array can it be employed in on-site computations.

SECTION 5

THE DECISION SUBSYSTEM

by

William Kilmer, Jay Blum and David Peterson

5.1 Goal

The goal of the work described in this section is the design of a decision computer for a robot. Such a computer should be capable of either interpreting what is the object that has been viewed by the visual system in terms of a small number of possible corresponding acts or deciding what is the most likely act that the robot should perform in response to not only visual but to all inputs. Eventually two computers may be developed to handle each of the two requirements, although, for the present, one is being designed that is sufficiently general to handle the needs of both.

A decision computer is used both to interpret objects as described in subsection 3.5 and to decide, as described in subsections starting with 5.4, what is the most likely act the robot should perform.

5.2 Previous Descriptions

The decision computer was originally described as a model of that part of the animal nervous system known as the core of the reticular formation.^(15,16) The model represents the spatial, not the temporal properties of this formation and is therefore called S-retic. While it began as a model of the biological structure, the long-range design goal was to make it a functioning engineering system such as that described in 5.1 above.

5.3 Simulation

The design of the computer consists of the analysis presented in this section and simulations performed on the Instrumentation Laboratory general-purpose digital computer. The first successful simulation was achieved in December 1965. Further simulations made it possible to adjust parameters so that the model converged to the correct act in each of about 50 test cases, and always in from 5 to 25 time steps.

5.4 Computer Design

The computer logic resembles a stack of poker chips (Fig. 5-1). Each poker-chip region, M_i , is a hybrid computer module which will be described in two stages. To understand the operation in general it is sufficient to see the input-output connections shown in Fig. 5-2. Detailed operation will be described with more detailed illustrations.

The decision subsystem is intended to act like an admiral who commits the ships and aircraft under his command to one act, trusting that fine perceptions and fine control are made at their centers of specialty and are accurate. The subsystem is thus broad in the domain of its command but exceedingly shallow in any specific area. It will commit the robot to an act which is a function of the information that has played upon it in the last minute or so. After commanding the robot to an act (for example, advance, turn right, turn left, right itself, perform an experiment, etc.) it will send out directives to control centers, tuning them to this task.

Its important features are that it must handle a vast amount of highly correlated input information and arrive at one of a small number of mutually exclusive acts in a dozen or so time steps and with minimal equipment. The crucial information as to what act the system has selected will then be used to control the inputs so as to increase the probability that the act will be continued.

In Fig. 5-1, the 42 input lines, γ_i , are connected to the modules in a several-to-all, but not all-to-all, fashion. The outer box represents the environment. A model of this environment is established by factors, σ_i , of the set Σ . The S_i represent sensors of this environment which feed highly (but nontrivially) correlated inputs, γ_i , directly into the decision system. At this stage of design, all σ_i and γ_i lines are binary.

There are twelve logic modules in the present design. The sets of lines P_i (only P_7 is marked) indicate the act preferred by module M_i . There are four lines in each set because the model is at present capable of four acts. The four lines carry the four components of a probability vector.

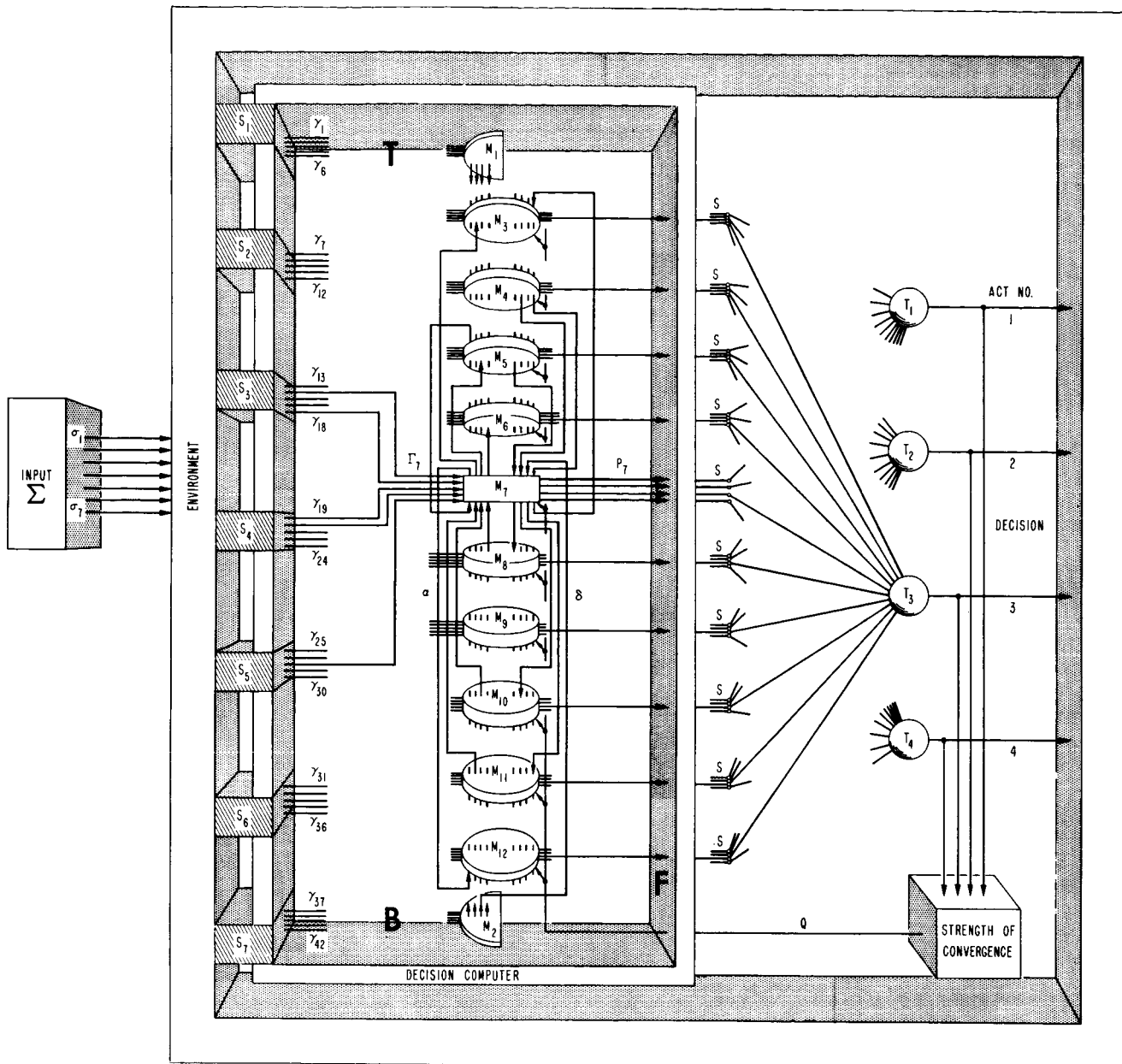


Fig. 5-1. Simulation of the decision subsystem.

For clarity, all types of connection lines (Γ , P , ascending and descending lines) are shown only for module M_7 , whereas these types of connection are actually made to all regular modules. Each M_i receives inputs from several but not all S_j , and each S_j feeds several but not all M_i .

5.5 Operation in General

Each module (Fig. 5-2) computes directly from the input information it receives and makes a best guess as to what the corresponding act probably should be. After the initial guess, the modules communicate their decisions to each other over low capacity information channels. Then each module takes the information (from all other modules) and combines it in a nonlinear fashion with the information coming directly into it to arrive at a mixed guess as to what act

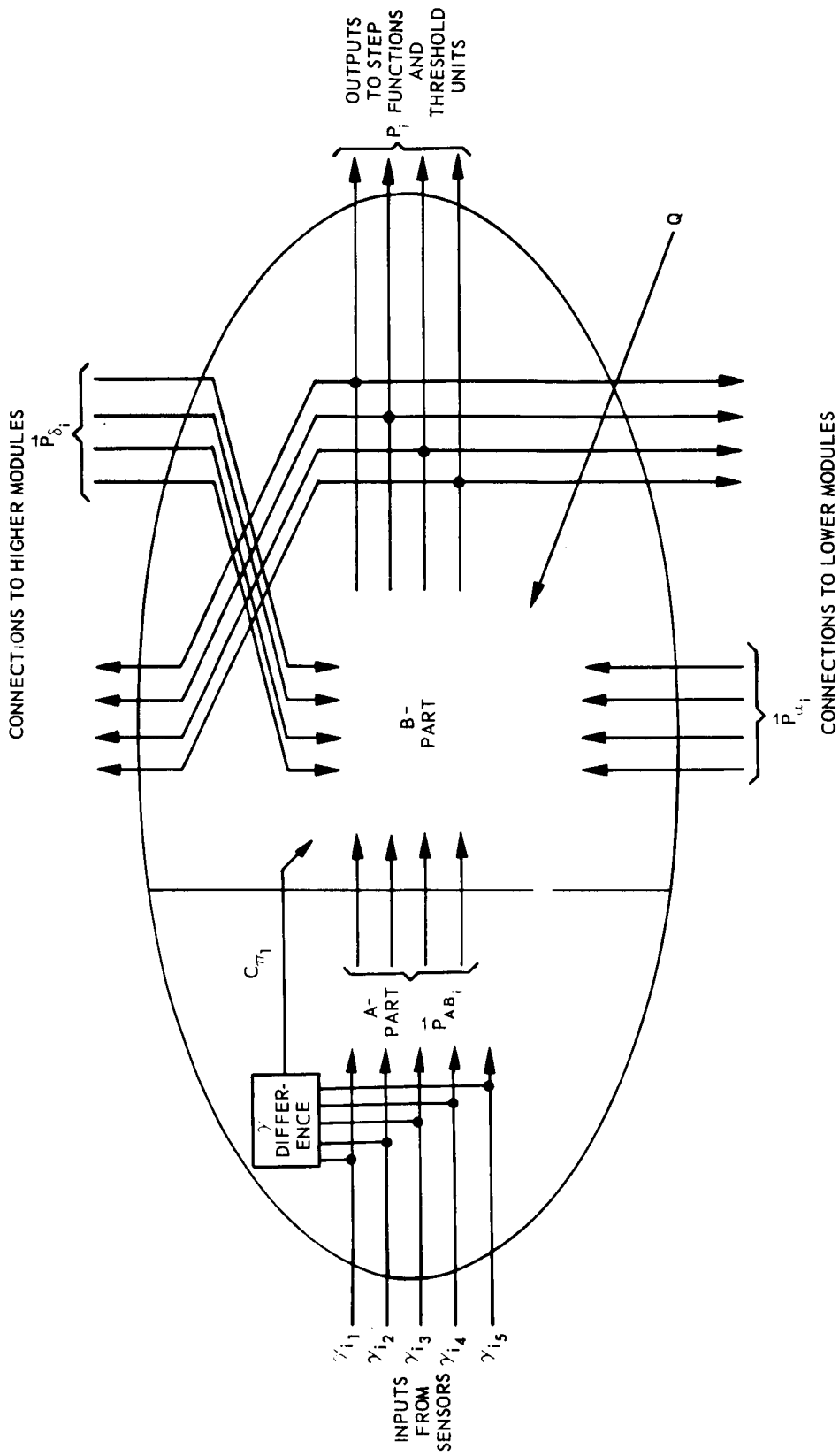


Fig. 5-2. Input and output connections to parts A and B of a module.

should be performed. This is in turn communicated to the subset of modules to which it is connected above and below. Thus we have decomposed the module shown in Fig. 5-2 into two parts. The A part operates on the module's input information. The B part operates on information from above, below and from the A part.

The A part with five binary input variables and four analog output variable outputs, is a nonlinear probability transformation network.

The B part receives 4-component probability vectors P_δ from the above, P_α from below and P_{AB} from the A part. The j^{th} component of each probability vector is the probability, computed by the module of origin, that the decision system's present γ input signal configuration demands act number j . The B part also receives the difference between γ inputs, called " γ difference" in Fig. 5-2 and the strength of convergence Q , shown being formed in the lower right corner of Fig. 5-1. The B part of each module yields the probability that the decision system's present γ input demands act number j .

The design of the modules was straightforward. The main problems concerned the way in which the computation converged to produce consensus. This consensus is achieved, as illustrated in Fig. 5-1, by first determining at point s if the j^{th} component of the probability vector P from each module exceeds 0.5. If it does, a 1 is passed on to the threshold element T_j . There, if 60% of the j^{th} component input connections are 1's, act j is decided upon. Note that each element T_j in Fig. 5-1 receives 10 inputs, although for clarity of the drawing, connections are shown only to T_3 . Each threshold element T is a crude model of a motor control subsystem which receives many inputs, decodes them and commands an act.

5.6 Definitions

A concept of importance in the decision system is that of the probability vector. A probability vector, associated with a decision for which there are n possible responses, is an n -component vector $\bar{P} = (p_1, p_2, \dots, p_n)$. Its j^{th} component, P_j , represents the probability that the j^{th} response is the appropriate one. For example, in the probability vector $P_1 = (0.35, 0.10, 0.15, 0.40)$, the probability is 0.15 that response 3 is the appropriate response.

A normalized probability vector is one representing mutually exclusive and collectively exhaustive responses; the components of such a vector thus sum to 1. The vector \bar{P}_1 in the example above is a normalized probability vector which can be represented:

$$\bar{P}_1 = \sum_{i=1}^n p_i = (0.35 + 0.10 + 0.15 + 0.40) = 1.0$$

In the present decision system, we consider 4 different responses, or acts; hence the probability vectors used in this report have 4 components.

A flat probability vector is one whose components are equal. A mean probability vector is a flat probability vector whose components are normalized. In general, the mean probability vector can be represented as

$$\bar{P}_m = (1/n, 1/n, \dots, 1/n)$$

n elements

The vector $\bar{P}_2 = (0.3, 0.3, 0.3, 0.3)$ is a flat probability vector while $\bar{P}_3 = (0.25, 0.25, 0.25, 0.25)$ is a mean probability vector.

The peakedness of a probability vector \bar{P} is a function proportional to the difference between \bar{P} and the mean vector \bar{P}_m . One definition of peakedness K of vector $\bar{P} = (p_1, \dots, p_n)$ is

$$K = \sum_{i=1}^n \left(p_i - \frac{1}{n} \right)^2$$

Other definitions of "peakedness" are used to meet the requirements of a particular case.

5.7 Detailed Operation

Given only its limited view of the environment, each module M_i ($i = 3, 4, \dots, 12$ in Fig. 5-1) computes, during the first time interval, the initial guess described in subsection 5.5. This is the normalized probability vector P_i . After all modules have made such computations, they communicate their respective P_i 's to each other over the low-capacity α - and δ -information channels (α and δ in Fig. 5-1). During the second time interval, each module combines in a nonlinear manner its own sense information about the environment with information coming into it from other modules to arrive at a finer-probability vector ("mixed guess" in subsection 5.5). This vector is communicated to the other modules, and during the third time interval, a yet-finer probability is computed. The system thus operates in cycles until the modules reach general agreement, or convergence.

At the completion of each cycle, the P_i output of each module is examined at s and then passed to the threshold elements $T_1 \dots T_4$. If the j^{th} component of P_i exceeds 0.5, the s passes a 1 to T_j . Otherwise, s passes on a 0. At T_j , if 60% or more of the inputs are 1's, then act j is decided upon. When an act has been selected, the box labeled "strength of convergence" sends back a Q signal to the modules. This signal is proportioned to the number of 1's received by T_z , where z is the act decided upon. Q prepares the modules for a new input by decoupling the modules from each other.

After a decision is reached, the system receives new $\Sigma = (\sigma, \dots, \sigma_7)$ and the entire decision process is repeated. If no decision is reached after a certain number of cycles, the system is reset and a new Σ requested.

Now that the decision system has been described, the internal structure of a module will be considered in detail.

5.8 Structure of a Module

There are two types of modules in the decision system. Modules M_3, \dots, M_{12} are "regular" modules. Modules M_1 and M_2 are "upper-lower" modules.

As previously explained, the regular module illustrated in Fig. 5-2 is divided into two parts. The A-part calculates a normalized probability vector \overline{P}_{AB} based upon the γ -inputs. The B-part produces a normalized probability vector \overline{P}_i as a function of both \overline{P}_{AB} and the probability vector \overline{P}_α and \overline{P}_δ from the other modules' B-parts.

The upper-lower modules consist of only A-parts. Their vector outputs \overline{P}_{AB} are distributed over α - and δ -lines to other modules, but are not used directly in making a decision.

The A- and B-parts are discussed separately in the following paragraphs.

5.9 The A-Part of Each Module

The A-part has two tasks. One is to determine when and by how much the input γ 's change. At the start of each cycle, the new γ 's are compared with the γ 's from the previous cycle. The parameter C_{π_1} is computed to be proportional to the number of γ 's that have changed since the previous cycle. Hence C_{π_1} is large when the outside world is changing dramatically, and small when the outside world is remaining essentially stable.

The second task of the A-part is to calculate a 4-component normalized probability vector P_{AB} based upon the γ -inputs from the senses. In the computer simulation of the nonadaptive decision system, the A-part is simply a tabular listing of Γ - to- \overline{P}_{AB} correspondence. The correspondences used were selected to represent situations in which the decision system has to make a choice. One possible adaptive A-part structure using threshold logic is presented in Appendix A. Another structure, using table-updating, will be presented in a subsequent memorandum.

5.10 The B-Part of Each Regular Module

Only the ten regular modules contain B-parts. Figure 5-3 shows the internal structure of each B-part. The inputs are C_{π_1} and \overline{P}_{AB_i} from the corresponding A-part, \overline{P}_δ from modules above M_i , P_{α_i} from modules below M_i , and Q from the

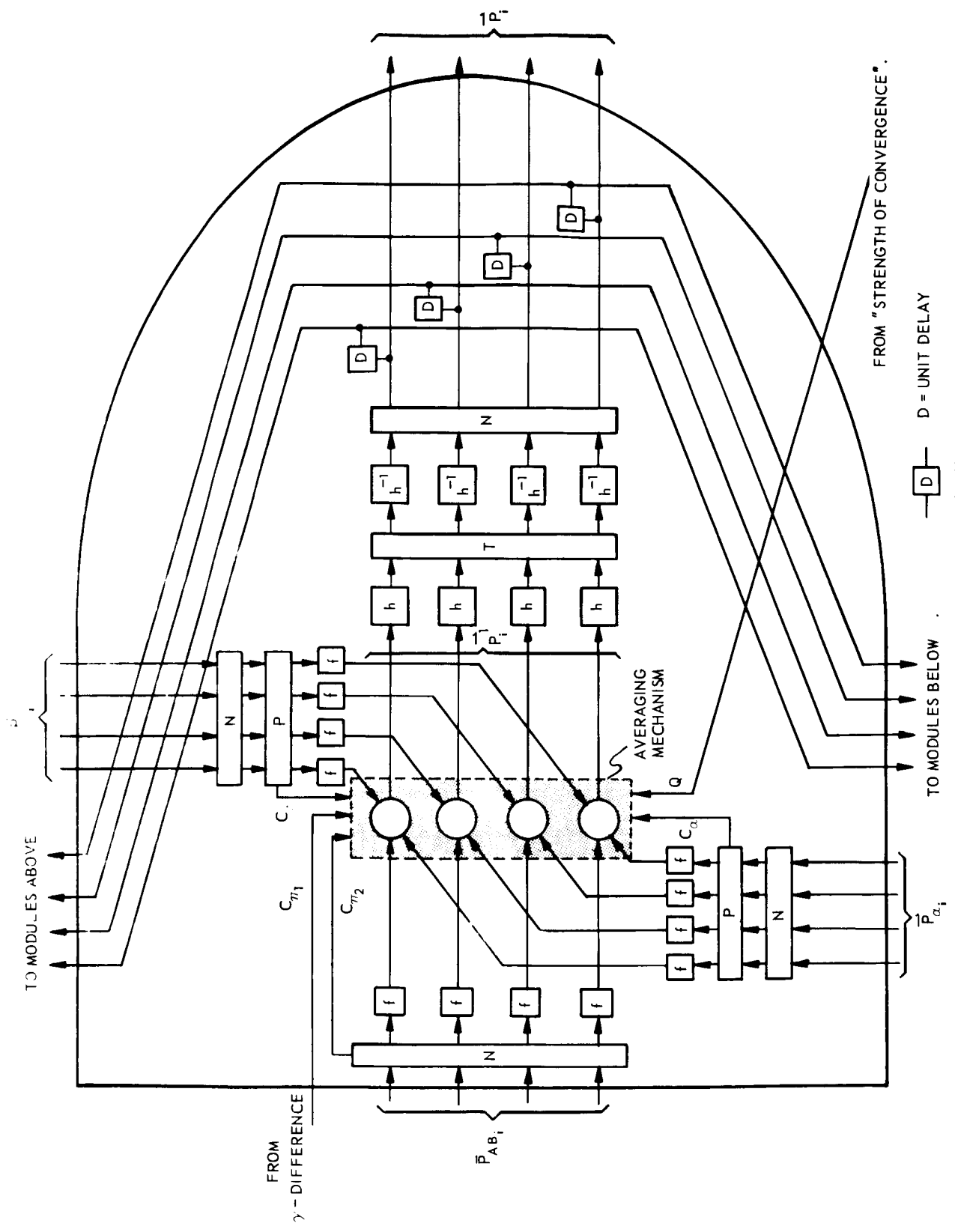


Fig. 5-3. The B-part of a typical module, M_i .

"strength of convergence". In general, each component of P_{δ_i} comes from a different module; similarly P_{α_i} .

Each of the boxes labeled "N" is a normalizer whose output is a normalized probability vector with components proportional to the corresponding components of the input probability vector. The boxes labeled "f" have the transfer characteristics shown in Fig. 5-4. The boxes labeled "P" calculate the peakedness of the respective input vector without changing the vector itself. C_α is the peakedness of the normalized P_{α_i} and C_δ the peakedness of the normalized P_{δ_i} .

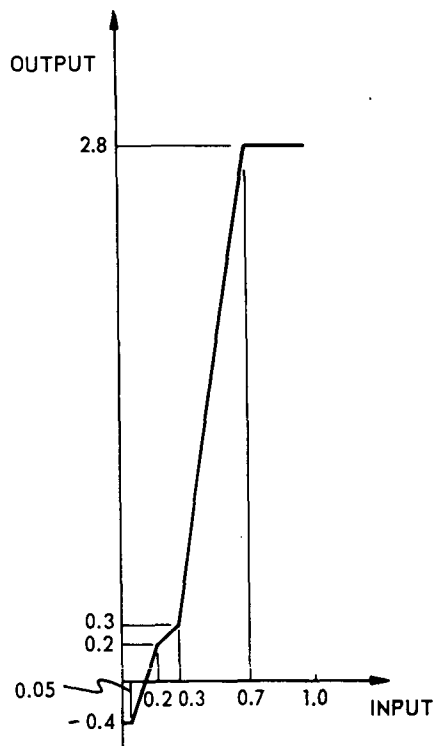


Fig. 5-4. The f function.

The averaging mechanism in Fig. 5-5 combines the \bar{P}_{AB_i} , \bar{P}_α , and \bar{P}_δ in a weighted average as follows:

$$\bar{P}'_i = \frac{C_{\pi_1} C_{\pi_2} Q f(\bar{P}_{AB_i}) + C_\alpha f(\bar{P}_\alpha) + C_\delta f(\bar{P}_\delta)}{C_{\pi_1} C_{\pi_2} Q + C_\alpha + C_\delta}$$

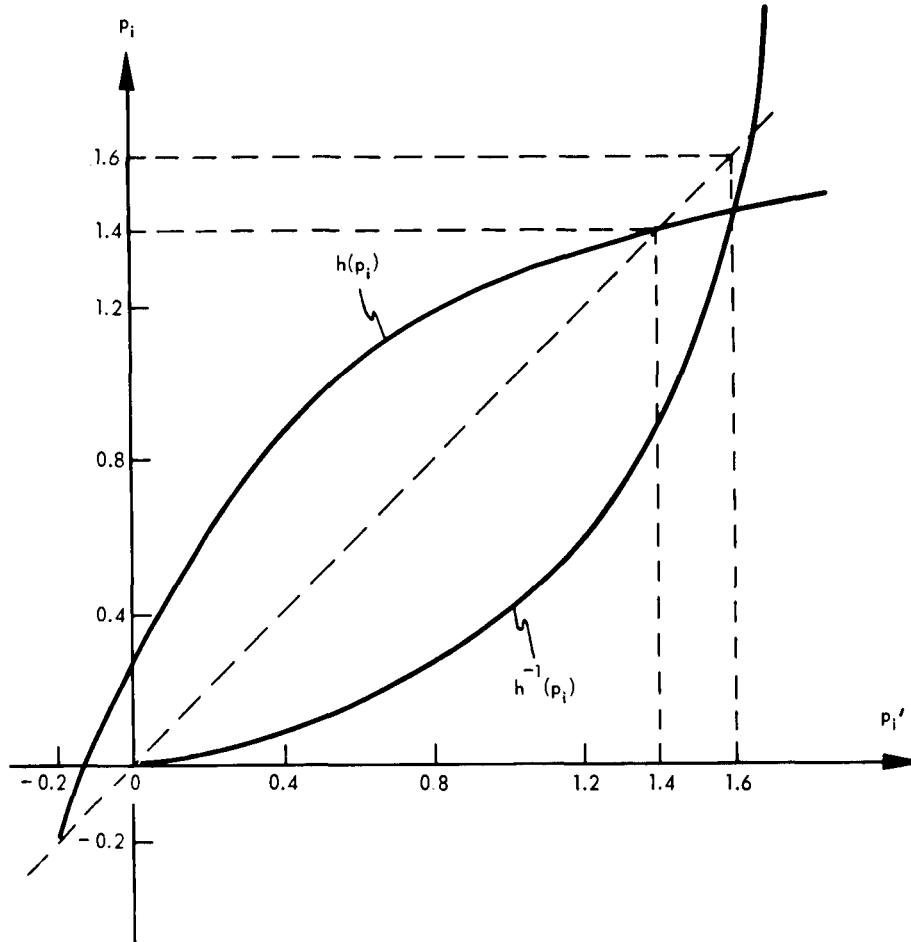


Fig. 5-5. $h(p_i)$ and $h^{-1}(p_i)$.

The preferences from the A-part of the module will be given more influence in determining \bar{P}_i' when C_{π_1} is large, i. e., when the outside world is changing dramatically. The preferences from the module above or below M_i will be given more influence when \bar{P}_δ or \bar{P}_α are very peaked.

In general \bar{P}_i' is not a probability vector in the true sense because the components of \bar{P}_i' are not all ≥ 0 . \bar{P}_i' must be restored to a probability vector while preserving the relative significance of the components. A single linear shifting of the components by adding an appropriate constant to each of them would yield a vector with positive components, but the relative meaning would be distorted, since difference between small probability components (e. g., between 0.25 and 0.05) are more significant than the same differences in magnitude between large

probability components (e. g. , between 0. 65 and 0. 85). Hence \bar{P}_i is first passed, componentwise, through an exponential function, h , as shown in Fig. 5-5. Then these components are linearly shifted into positive value in the "T" box (Fig. 5-3) by adding to each component the absolute magnitude of the most negative component. The results of the shifting are then passed componentwise through the h^{-1} curve (Fig. 5-5) and normalized at N , resulting in the module's output vector \bar{P}_i . This is sent to specified modules above and below M_i after a unit delay.

SECTION 6

CONCEPTUAL MODEL OF THE FROG'S TECTUM

by

Roberto Moreno-Diaz

6.1 Introduction

The model of a frog's visual system described in previous reports^(3,5) has been extended to include a model of the tectum.

Figure 6-1 is a diagram of the frog's visual system with the eyes enlarged so that the ganglion cells can be illustrated collecting information from the retina and conveying it to both the optic tectum and the geniculate nucleus. Connections to the tectum are the principal ones. Experiments indicate that only the presence of blue light in the field of view is reported to the geniculate.

Figure 6-2 represents schematically the retina and optic tectum. The retina consists of three layers: photoreceptors, bipolar and ganglion cells. The photoreceptors, which respond to light, stimulate the bipolar cells, which in turn stimulate the ganglion cells, whose axons, or tails, comprise the optic nerve. The axons of each of four kinds of ganglion cells terminate on four separate layers of the tectum. Each type of ganglion cells performs a different analysis of the retinal image and reports, through the optic nerve, to the tectum, in the following manner:

1. Group 1 ganglion cells respond to edges, i. e. , to differences in illumination on the receptive field.
2. Group 2 ganglion cells respond to the image of a small dark object, moving centripetally into its visual field.
3. Group 3 ganglion cells respond to any change, spatial or temporal, in the luminance of the scene.
4. Group 4 ganglion cells respond to dimming of light.

Lettvin, et al. have found correlation between the form and function of each of these cells.⁽¹⁷⁾

Their description of the tectum has not been as thorough, however, since they were concerned only with the response of tectal cells in an animal acquiring

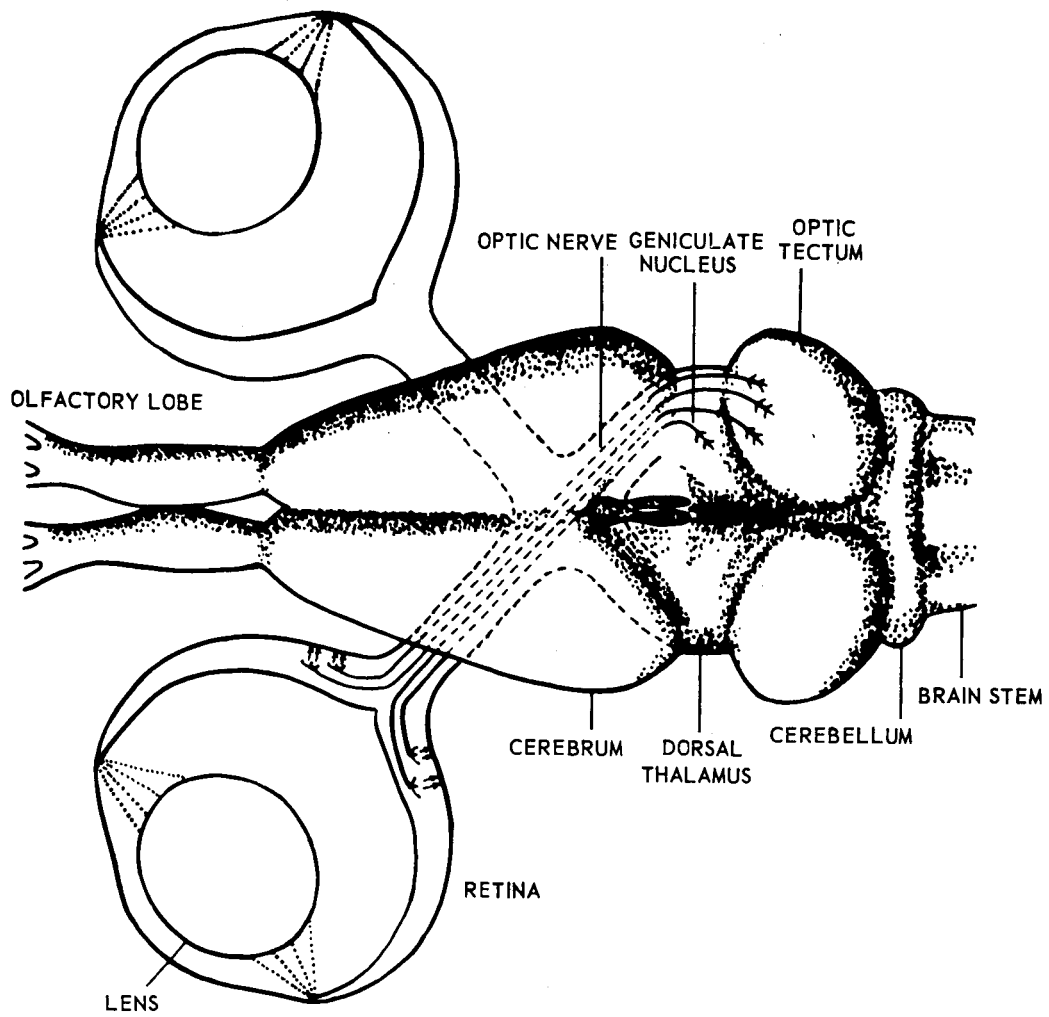


Fig. 6-1. Diagram of frog's visual system.

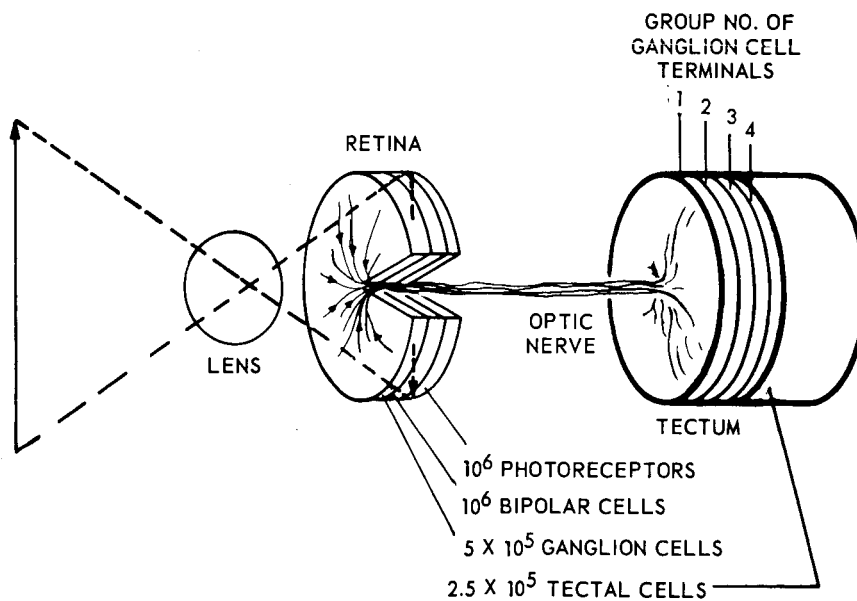


Fig. 6-2. Schematic of frog visual system.

food⁽¹⁷⁾ Nevertheless, theirs is the only description of tectal behavior suitable to be considered in our model.

6.2 Neurophysiological Basis of the Model

Pedro Ramon y Cajal's drawing of the frog's tectum is shown in Fig. 6-3. Although the drawing is not correct in detail, there are four main features that

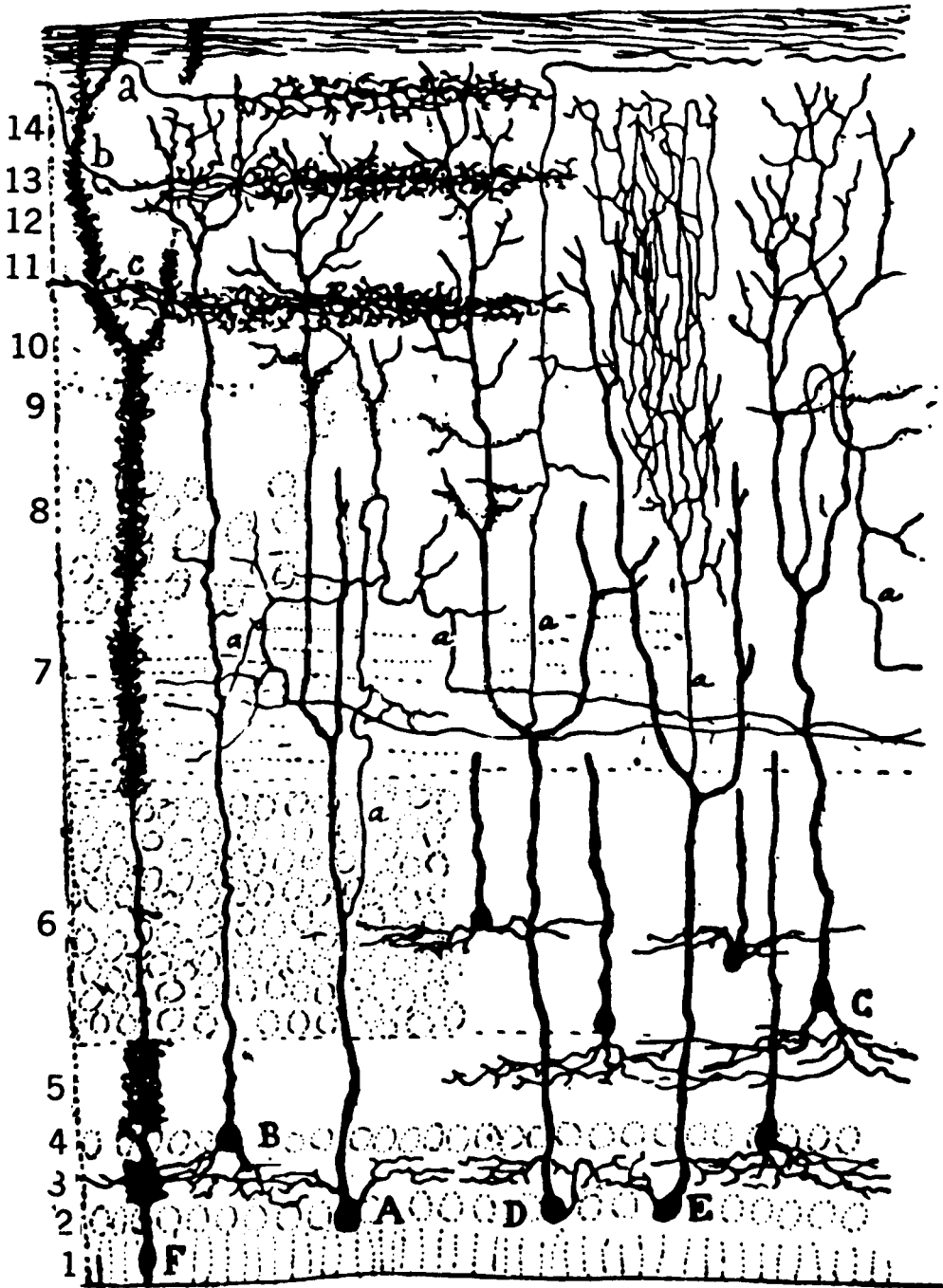


Fig.6-3. Pedro Ramon y Cajal's drawing of optic tectum in the frog.

appear clearly. First, the cell bodies lie in the deeper layers (1 to 6 in Fig. 6-3). Second, the neurons seem to have a restricted dendritic tree. Third, axons leave the tectum branching from a main ascending dendrite. Fourth, interconnections among cells lying at the same depth is strongly suggested.

Figure 6-4 adopted from the discussions of Ref. 17 shows what appear to be the essential anatomical features of the tectum. Axons from the four major retinal ganglion cell groups enter the tectum as the optic tract and map onto the four superior tectal layers called the superficial neuropile. Axons from ganglion cells which respond to adjacent retinal areas map onto adjacent points in the neuropile. Thus, each small area in the retina corresponds to four small areas, one on each layer, in the neuropile. Within the neuropile there also exist a few cells – not represented in the figure – which appear to be lateral connectives.

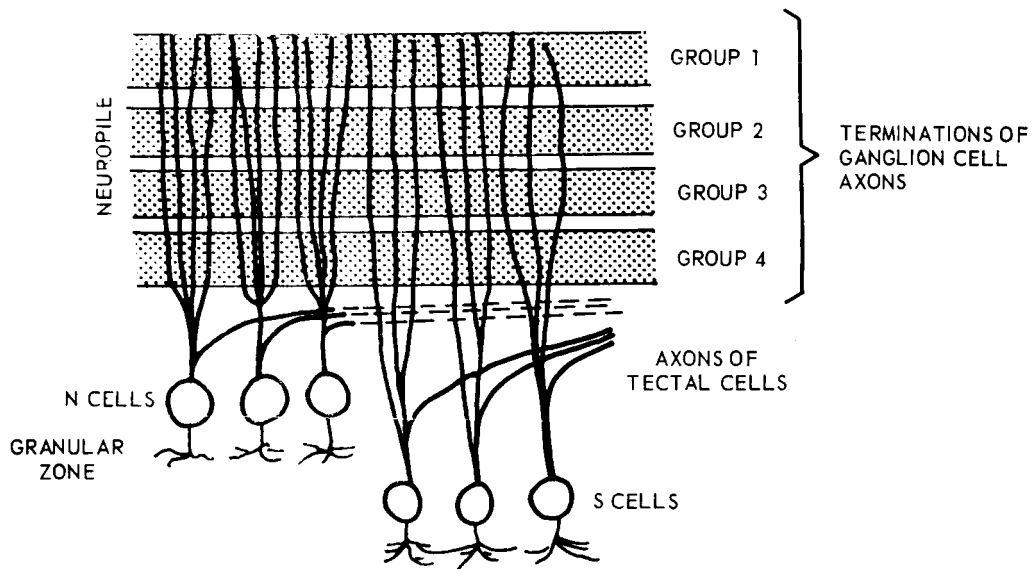


Fig. 6-4. Simplified diagram of frog's tectum.

All other tectal cell bodies lie in the granular layer, beneath the superficial neuropile (Fig. 6.3). Their dendrites, which have the appearance of columns, extend up through the four neuropile layers covering a small area in each layer. Their axons leave the tectum by branching from the main dendrites, at the lower part of the neuropile.

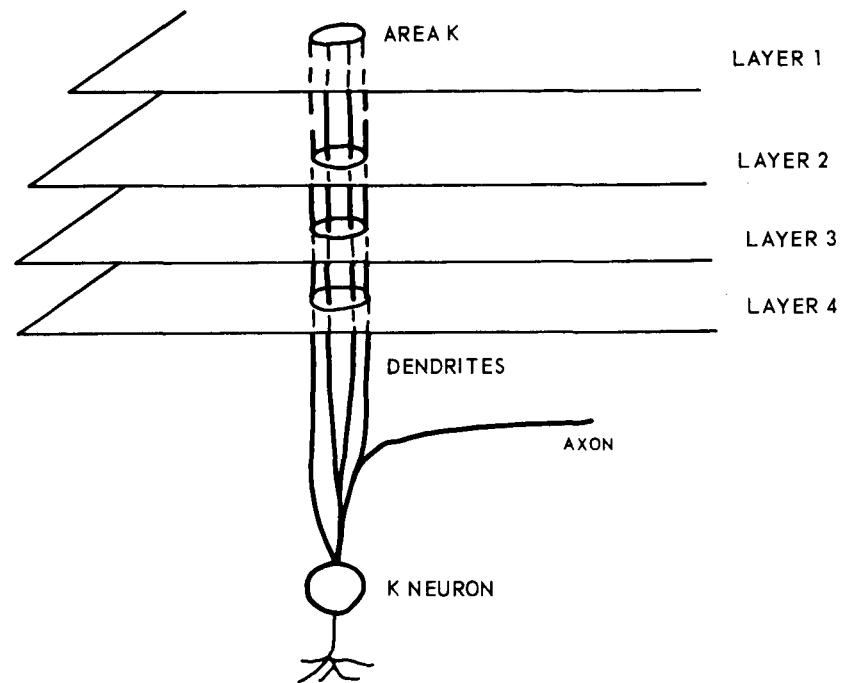


Fig. 6-5. Diagram of a tectal neuron.

Lettvin, et al. have distinguished from several varieties of tectal neurons two extreme types: "Newness" cells, N, sensitive to new objects in the visual field, and the "Sameness" cells, S, sensitive to the same object for a specific period of time. The bodies of Sameness cells lie deep in the granular zone.

The properties of Newness and Sameness cells are shown by the following outline:

a. Newness Cell

1. Its receptive field is approximately 30° in diameter, with considerable overlap.
2. It yields small responses to sharp changes in illumination.

3. Its response frequency increases if the motion of an object is irregular. Its response also depends on the velocity and size of the object and on the direction of motion.
4. It has no enduring response.
5. Its adaptation time is less than 1 second.
6. Adaptation is erased with a step to darkness.

b. Sameness Cell

1. Its receptive field is almost all the visual field, but includes a null region.
2. It does not respond to changes in illumination.
3. It responds to the presence of an object in its field by generating a low frequency pulse train. Response is maximum to objects about 3° in diameter.
4. It "notices" with a "burst" of pulses all motion discontinuities. It discriminates among objects, fixing its "attention" on the one with the most irregular movement.

Lettvin, et al, comment that N and S cells may be considered two extremes of several types of tectal cells. From Pedro Ramon y Cajal's drawings, tectal cells do not seem to be significantly different, anatomically, although S cells could receive excitation from N cells. A general tectal model could be envisioned, in which N and S cells would be differentiated only by values of parameters, such as adaptation time, width of the receptive field, etc. This is the point of view adopted here.

While the receptive field is relatively wide for both types of cells, the dendritic tree is very restricted. Interaction between tectal cells would account for this observation.

6.3 Conceptual Model

In the conceptual model of tectal-cell behavior, object velocity and size is determined by signals assumed to originate on the retina. For convenience these current and voltage signals are referred to simply as "activity".

Assume that each layer of the superficial neuropile is divided into small areas, such as area K in layer i ($i = 1, 2, 3, 4$). (See Fig. 6-5.) Some ganglion-cell axons of Group i map into this area and emit their signals there. Assume a decoding process which produces analog values such as voltage signals. Let $V_{iK}(t)$ be the voltage signal indicating the response of the ganglion cells which map into area K of layer i.

Assume further that the dendrites of each tectal neuron are restricted to an area K - i. e. , there is no overlapping. The first process that is suggested is a summation of the signals, $V_{iK}(t)$, for the same K and different i 's at time t . A simple linear combination is postulated:

$$V_K(t) = \sum_{i=1}^4 \alpha_{iK} V_{iK}(t) \quad (1)$$

The coefficient α_{iK} may be either positive or negative and is assumed constant. If it is positive, the corresponding $V_{iK}(t)$ is said to be excitatory; if it is negative, $V_{iK}(t)$ is said to be inhibitory. α_{1K} , α_{2K} and α_{3K} are positive, whereas α_{4K} is negative. By summation⁽¹⁾ a series of "vertical" lines is obtained, which transmit signals $V_K(t)$ through the superficial neuropile. These signals interact due to the conductivity of the medium through which they pass.

Four interaction processes account for tectal cell properties. (See Fig. 6-6.) Process A at the level of the dendrites, and Process D, at the level of the axons, are of the same nature - i. e. , an interaction due to the conductivity of the medium. Process B, which accounts for adaptation, may be produced by the existence of a distributed capacity which, once charged, damps the transmission of the signals. Process C requires non-symmetric elements (e. g. , diodes) that could be provided by the cellular membrane. These processes are described in more detail in the following subsections.

6.4 Interaction Process A (Facilitation)

Lateral spreading of activity increases the response to an irregularly moving object. $V_K(t)$ is referred to as the initial activity of line k , i. e. , the signal before interaction. Its effect on another line j depends upon the distance d_{kj} according to a continuous and decreasing function $f(d_{kj})$; $f(d_{kj})$ is such that as $f \rightarrow 0$, $d_{kj} \rightarrow \infty$. This effect propagates with a velocity, γ , assumed to be constant. It is further assumed that the effects of different lines on a particular one add linearly. Therefore, the final activity (i. e. , activity after interaction), $V'_K(t)$, is:

$$V'_K(t) = V_K(t) + \sum V_j \left(t - \frac{d_{kj}}{\gamma} \right) f(d_{kj}) \quad (2)$$

where the sum is over all lines except k . If $f(0) = 1$, Eq. (2) becomes:

$$V'_K(t) = \sum V_j \left(t - \frac{d_{kj}}{\gamma} \right) f(d_{kj}) \quad (3)$$

where the sum is over all lines, including k .

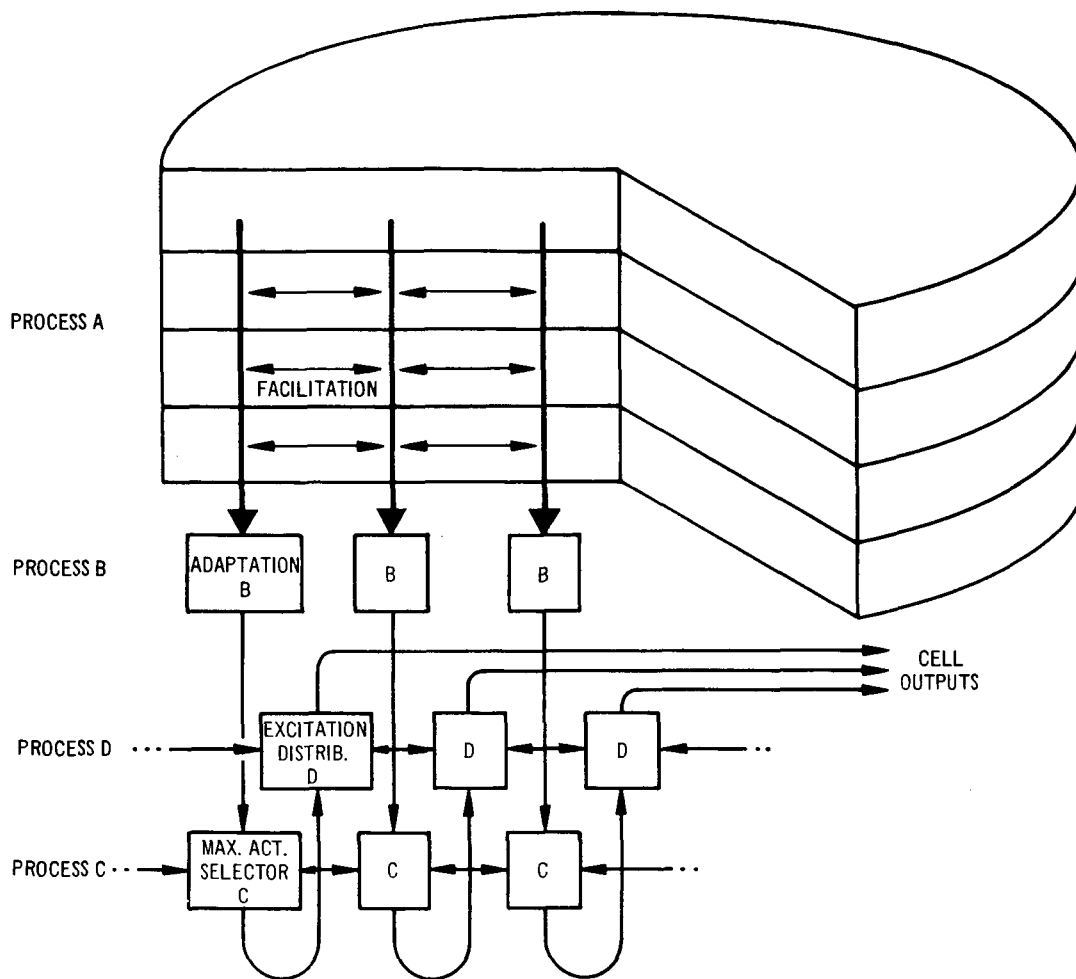


Fig. 6-6. Diagram of tectal cell interaction processes.

Lateral coupling is assumed for Type N neurons over a zone covering 30° of the visual field; for Type S, over the entire visual field.

Figure 6-7 shows an example of the results of this interaction for an object following a straight path. The distribution of equipotential activity shows that the summed voltage will be greater for objects that change their direction of motion.

6.5 Interaction Process B (Adaptation)

Proper capacitive coupling will cause a line that has been excited to adapt and damp any further transmission for some time. Appropriate capacitors are described in subsection 6.8.

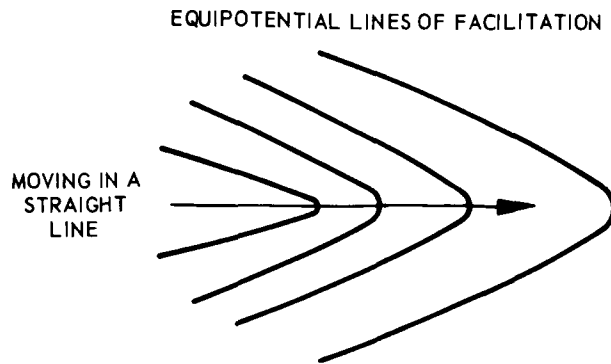


Fig. 6-7. Facilitation for an object following a straight path.

6.6 Interaction Processes C and D (Maximum-activity selection and distribution)

Process C blocks all paths except the one having maximum activity, and Process D distributes this activity to the other lines, in a manner similar to Process A. The following circuit analogy provides an example that helps understand how these processes can be realized. Assume a number of generators, each with a voltage $V_K^i(t)$ connected through an ideal diode represented by a diode in a circle in Fig. 6-8. Currents flow through axonal resistors $R_{ax,K}^*$ from the $V_K^i(t)$ with the highest value. Neurons belonging to the zone where this type of interconnection exists will follow that with the highest activity. Thus, the $V_K^i(t)$ with highest value will appear to "govern" the others. If there exist two objects in the field of view corresponding to the zone in question - i. e., two generators with a high value - only that which produces the higher $V_K^i(t)$ will be followed.

If it is now imagined that some coupling resistors exist (indicated by dots in Fig. 6-8), the action of $V_K^i(t)$ will be attenuated with an increase in the distance from the area that produces it. Information concerning the position of the object in the field of view will be maintained in the RC circuits.

6.7 Parameters of Types N and S Neurons

With lateral coupling for Type N neurons assumed for a zone covering 30° of visual field, necessary capacitive time constants for adaptation are such that damping of signals occur in 1 second and persist for 50 to 70 seconds. The

*The output of the tectal cell, K, could be regarded as a pulse train of a frequency proportional to the current through $R_{ax,K}$.

difference between the time required for adaptation and the time for erasure of adaptation is a consequence of the nonlinear elements (diodes) that cause Process C, if we assume that they are real diodes; i. e., they have a finite, although high, backward resistance. This assumption will not modify appreciably interaction Process C as long as the backward resistance is orders of magnitude higher than R_{ax} . As stated in subsection 6.3, V_{1K} , V_{2K} , and V_{3K} are positive whereas V_{4K} is negative. As a result, adaptation is erased by a step to darkness – i.e., strong firing of Group 4 ganglion cells – the capacitors are then discharged through the backward resistance of the diodes.

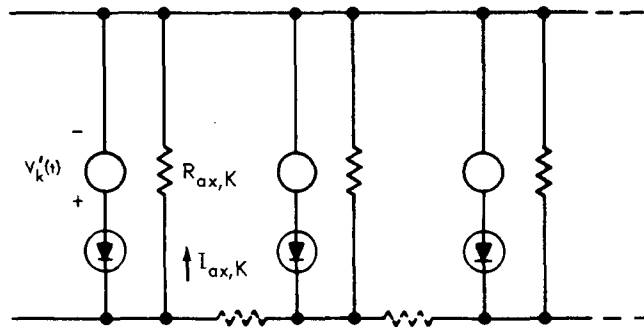


Fig. 6-8. Equivalent circuit of Processes III and IV.

For Type S neurons, $V_K(t)$ is made higher by the addition to the signals coming from the retina of the output of some Type N neurons. For Type S cells lateral coupling occurs over almost all the visual field. Adaptation is negligible, implying a high value for the adaptation capacitance.

6.8 Equivalent Circuit of a Group of Tectal Cells

The circuit analog of a group of either Type N or S tectal cells is shown in Fig. 6-9. The group includes only those cells which are situated at the same level in the granular layer. Process A is not indicated. C_K is the equivalent capacity for adaptation. $D_{r,K}$ is a real diode. Interaction among the axons of neurons belonging to the same group is indicated by resistors R_C . The rate of firing of a cell is considered to be proportional to $(I_{ax,K} - \theta_K)$, where $I_{ax,K}$ is the current through $R_{ax,K}$ and θ_K is a fixed threshold. The directionality of some cells can be explained by assuming an asymmetric distribution in the values of the coupling resistances R_C .

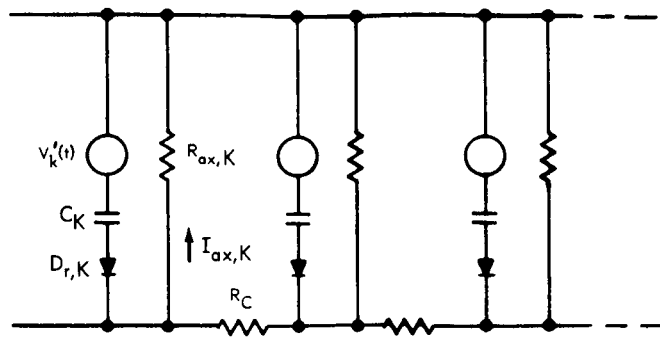


Fig. 6-9. Equivalent circuit of a group of tectal cells.

6.9 Discussion

The main properties of tectal cells are accounted for in a simple manner by the model. Insufficient neurophysiological data does not permit any further approximation. As a recapitulation, the main hypotheses of the model are as follows:

- a. The same basic mechanism is assumed for both Types N and S cells. To produce the desired response for the cells, this mechanism should include the four processes described in subsection 5.3, namely, lateral facilitation, adaptation, selection of maximum activity, and distribution of it.
- b. The electronic equivalent circuit of Fig. 6-8 illustrates three of the four postulated processes.

APPENDIX A

NOTE TO SECTION 4: IMPLEMENTATION OF THE A-PART OF A DECISION-SYSTEM MODULE USING THRESHOLD LOGIC

Figure A-1 is a schematic diagram of an A-part using threshold logic. The e_k are linear threshold logic elements. The gains, or weights, a_{jk} can be either positive or negative. For threshold a_{jk} , the output v_{ik} of threshold element e_k is

$$v_{ik} = \begin{cases} 1 & \text{for } \sum_{j=1}^5 a_{jk} \gamma_{ij} \geq a \\ 0 & \text{for } \sum_{j=1}^5 a_{jk} \gamma_{ij} < a \end{cases} \quad (1)^*$$

Each f_l in Fig. A-1 is a summation element whose output is

$$P_{AB}_l = \sum_{k=1}^m w_{kl} v_{ik} \quad (2)$$

This threshold and summation logic approach can incorporate learning through the reinforcement of the weights a_{jk} and w_{kl} as a result of rewards fed back from the environment.

*Thus, v_{ik} is equal to 1 when the sum of each of the inputs γ_{ij} times its respective weight a_{jk} is equal to or greater than the threshold a . Otherwise v_{ik} is equal to 0.

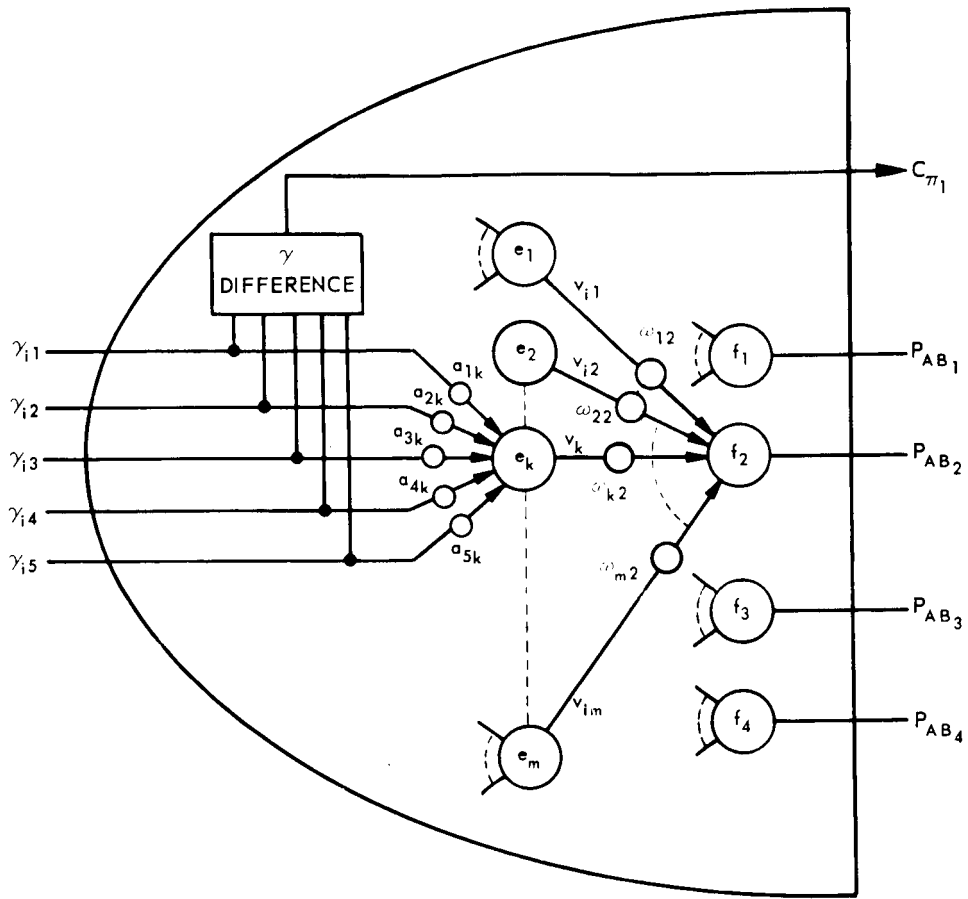


Fig. A-1. Threshold logic implementation of the A-part of module i.

LIST OF REFERENCES

1. Sutro, L.L., Moulton, D.B., Warren, R.E., Whitman, C.L., Zeise, F.F., 1963 Advanced Sensor Investigations, R-470, Instrumentation Laboratory, Massachusetts Institute of Technology, Cambridge, Massachusetts, September, 1964.
2. Sutro, L.L., editor, Advanced Sensor and Control System Studies, 1964-September, 1965, R-519, Instrumentation Laboratory, Massachusetts Institute of Technology, Cambridge, Massachusetts, January, 1966.
3. Sutro, L.L., Information Processing and Data Compression for Exobiology Missions, R-545, Instrumentation Laboratory, Massachusetts Institute of Technology, Cambridge, Massachusetts, June, 1966.
4. Mahoney, J.J., Data Transmission Capabilities of Mars Probes and Landing Capsules, American Astronautical Society, Anaheim, California, May 23-25, 1966.
5. Moreno-Diaz, R., An Analytical Model of the Group 2 Ganglion Cell in the Frog's Retina, E-1858, Instrumentation Laboratory, Massachusetts Institute of Technology, Cambridge, Massachusetts, October, 1965.
6. Sutro, L.L., Information Processing and Data Compression for Exobiology Missions, R-545, p. 5-12.
7. Bendix Systems Division, Surveyor Lunar Roving Vehicle, Interim Study, Final Technical Report, BSR 1096, the Bendix Corporation, Ann Arbor, Michigan, February 1, 1965.
8. General Motors Research Laboratories, Final Report, Surveyor Lunar Roving Vehicle, TR 64-26, General Motors Corporation, Santa Barbara, California, April 23, 1964.
9. Ibid., p. 13-15.
10. Malling, L.R., Space Astronomy and the Slow-Scan Vidicon, Journal of the SMPTE, Volume 72, November, 1963.
11. Sutro, L.L., editor, Advanced Sensor and Control System Studies, 1964 to September, 1965, R-519, p. 61-64.
12. Schuster, M.A., and Strull, G., A Monolithic Mosaic of Photon Sensors for Solid-State Imaging Applications, IEEE Transactions on Electronic Devices, December, 1966.
13. Broderick, J.C., and Schuster, M.A., A Molecular Camera for Aerospace Applications, 1965 International Space Electronics Symposium, Miami Beach, Florida, November, 1965.
14. Fink, D.G., Television Engineering Handbook, McGraw-Hill, p. 1-50, 1957.
15. Sutro, L.L., editor, Advanced Sensor and Control System Studies, 1964 to September, 1965, R-519, p. 84-95.

LIST OF REFERENCES (Cont.)

16. Sutro, L. L. , editor, Advanced Sensor and Control System Studies, 1964 to September 1965, R-519, p. 84-95.
17. Lettvin, J. Y. , et al. , Two Remarks on the Visual Systems of the Frog, Sensory Communications, W. Rosenblith, ed. , Massachusetts Institute of Technology, 1961.
18. Nathan, Robert, Digital Video Data Handling, Technical Report No. 32-877, Jet Propulsion Laboratory, California Institute of Technology, Pasadena, California, January 5, 1966.